INTRODUCTION

The Talbot effect is a near field diffraction effect that has been observed both with light and with atom optics. The origins of this effect, the conditions necessary for it to occur, and some possible applications are the subject of this paper. When a plane wave is transmitted through a grating or other periodic structure, the resulting wave front propagates in such a way that it replicates the structure at multiples of a certain defined distance, known as the Talbot length. Right away one can see potential applications. An existing periodic structure can be used in conjunction with light waves or atom waves to create a replica of the structure a Talbot length away. However, the details of the Talbot effect bring out the most interesting possible applications. Exactly halfway between these locations, the Talbot effect reproduces the structures with half the spatial period of the original structure. As one might imagine, the story does not stop there. The Talbot effect will produce smaller fractional revivals under perfect conditions. Thus, it is not surprising that the intensity pattern as a function of propagation distance away from a periodic structure is often referred to as a Talbot carpet.

This behavior suggests the possibility of Talbot-assisted lithography, in which the wave nature of the atom is utilized to create very small structures. Specifically, it could lower the current size limit for which a regular pattern of any two-dimensional shape can be produced. For example, it would be conceivable to place a substrate 1.5 times the Talbot length away from a physical grating with a 100 nm period, and deposit rows of atoms spaced 50 nm apart onto this substrate. The rows of atoms could form 20 nm wires, which is 6 times smaller than the features on a Pentium 4 chip.[1] Of course, there are limits to how small these structures can get. First of all, the contrast of the revivals is

not perfect, and decreases with the size of the fractional period. Also, since perfect conditions are never achieved, the actual revival behavior will be strongly influenced by factors such as the wavelength distribution, interactions between the waves and the grating structure, and beam collimation. This paper will examine the possibility of such quantum lithography both theoretically and experimentally by taking into account some of these limiting factors.

HISTORY

The Talbot Effect was discovered by its namesake, Henry Fox Talbot, in the mid-eighteen hundreds. Talbot was born February 11, 1800 in Dorset, England, and studied mathematics and classics at Cambridge. After being elected a Fellow of the Royal Society in 1832, he worked to produce images that would stay fixed on a piece of paper. These experiments resulted in his fame, as he is now known as one of the inventors of photography.[2] During his studies he observed the remarkable effect that now carries his name. When he examined a coarsely ruled diffraction grating with a simple magnifying lens, Talbot noticed that the grating image would reappear as he moved the glass out of focus. If illuminated by white light, it would split into different colors, and monochromatic light would cause the image to come into focus at multiples of a particular distance. Talbot published the results of some of his experiments on the subject in 1836, but did not pursue the subject further, as he was investing his time and money into photography. The Talbot effect was forgotten, until it was rediscovered by Lord Rayleigh in 1881. Rayleigh explained it as a natural consequence of Fresnel diffraction, and showed that the Talbot length z_T is given by

$$z_T = \frac{a^2}{\lambda}$$

where a is the period of the grating and λ is the wavelength of the incident light. He also mentioned that the Talbot effect could have a practical application to reproduce gratings by exposing film to one of the revival images behind the original grating.[3] Had Rayleigh known of the wave-nature of atoms, he probably would also have suggested the technique for atom lithography.

CREDIT WHERE CREDIT IS DUE

The Talbot effect for matter waves has also been studied extensively in the last 20 years. At least 30 scientific papers have been written on the topic, ranging from the purely theoretical side to applications thereof. One paper that specifically focuses on matter-wave diffraction due to near-field grating sequences contains in-depth and extensive Fourier optics approaches to describing these atom-optical situations.[4] On a more experimental note, there have been several direct observations of the atomic Talbot effect. One of the first of these strongly supports the feasibility of this project and became part of the reason it was undertaken. In 1993, Michael Chapman and others used a simple two-grating setup to demonstrate the Talbot effect with atom waves. The first grating creates the Talbot carpet, and the second grating of equal periodicity and orientation functions as a mask. When the second grating is located a Talbot length behind the first and gets scanned in the direction transverse to the beam, the transmitted intensity oscillates.[5] The other, by Nowak et al., used a single grating and a narrow detector that scanned out the whole Talbot carpet. The fractional revivals of the grating were also clearly seen, with significant contrast even for the 1/5 and 1/6 period revivals.[6] Both of these papers mention the possibility for using this effect as a method for atom lithography. However, to this date no paper describes using the Talbot effect with atom waves to directly deposit atoms onto a surface.

Of course, atom lithography is not the only conceivable practical use of the atomic Talbot effect. Some others include a Talbot-von Lau atom interferometer[7] and distance measurement utilizing the Talbot effect.[8] Atom lithography, however, does

receive very much attention because of its usefulness in creating structures smaller than today's computer chip features. A related method for atom lithography utilizes atom diffraction through an optical grating. The atom beam travels through an optical standing wave, which acts as an array of cylindrical lenses i.e. a periodic phase-mask for atom waves. A number of research groups have illustrated this method with great success. A group led by Prentiss and Timp first succeeded in showing this effect in 1992.[9] Three years later, McClelland *et al*. used a standing wave to deposit rows of chromium atoms with a 212.78 nm period onto a surface, which corresponds to the fundamental period of the optical grating of $\lambda_{laser}/2$.[10] Rehse *et al.* did the same in 2000 with aluminum, and achieved a periodicity of 155nm using resonant 310nm light.[11] Although the method is attractive because of the relative ease with which such an optical grating is produced, it does have its drawbacks. First of all, the line spacing is fixed at half the wavelength of the laser light, due to the nature of a standing wave. One could conceivably use fractional Talbot revivals with such a standing wave, but the contrast decreases quickly, and the few revivals that would produce enough contrast will still be linked to a light wavelength. This puts a limit on grating period as defined by the available optical wavelengths. Also, since the atoms have to be nearly on resonance with the light, the laser's frequency must be tuned to a frequency specific to the depositing atoms. Therefore, the line spacing not only has a quite large lower limit, but is also constrained by the type of atoms used. Finally, the shape of the resulting structures is severely limited. McClelland *et al.* shows that the technique can be modified to create an array of dots, but not much can be done beyond that to create a specific shape.

Nanostructure fabrication through the use of a physical grating offers more possibilities by avoiding these problems. The physical grating will work regardless of the types of atoms (or even molecules) used as long as the van der Waals interaction between the matter wave and the grating is not excessive, which I will discuss later in the paper. High quality physical gratings of 100 nm periods are already available, so the size limit is already an improvement, even if no fractional revivals are utilized. Yet arguably the greatest benefit over standing optical waves is the freedom to make an arbitrary shape.

THE OPTICAL TALBOT EFFECT

Before searching for the atomic Talbot effect, I investigated the much more accessible optical Talbot effect to get a feel for how it works. The first setup we used was an optical microscope with a digital camera attached. We imaged one of the nanostructure gratings used in the atom interferometry experiment. Of course, it was impossible to optically image the actual grating bars because their 100 nm periodicity is smaller than the resolution of an optical microscope. However, the support structure for these bars made up another grating with a 2 μm period, which was easily visible through the microscope. As the grating was moved out of the focal plane, the image reappeared as expected. It was even easy to see the half-period revival at the intermediate positions. These pictures are shown in figure 1.

Fig. 1

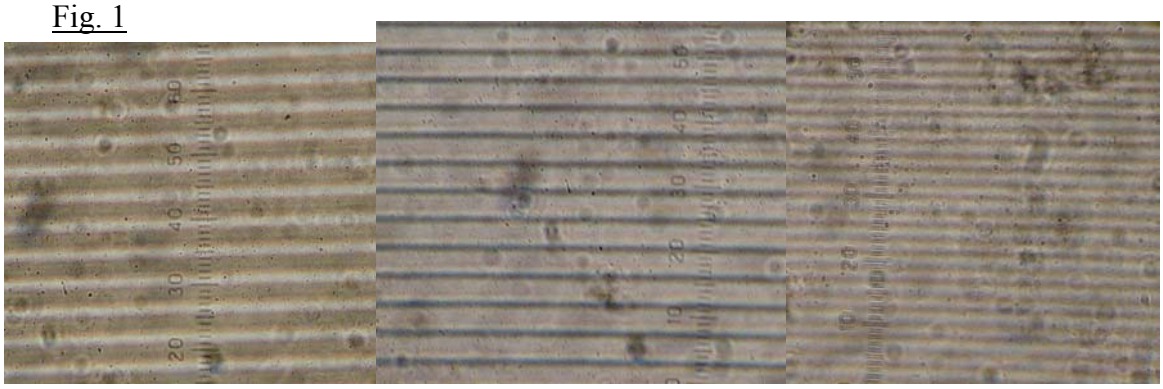

For the next step I used a Ronchi rule and laser setup. Using simple far-field diffraction and measuring the positions of the bright bands, the grating's periodicity measured to be about 6 lines/mm. The laser used was a simple diode laser pointer, which was labeled as 650 nm. In order to see the results more clearly and illuminate more grating bars, a beam expander was put in front of the laser. Since the individual lines of

the Ronchi rule were still visible to the naked eye, a screen placed behind the grating easily illustrated the Talbot effect. By placing the screen at an angle to the beam to "stretch out" the spot, the half-period revivals became easily visible. According to the formula for Talbot distance, $z_T = 4.1$ cm. However, because the diode laser frequency is unlikely to be exactly 650 nm, and since it was used both directly in the formula and to measure the grating period, it is expected that the actual Talbot length would be a bit different. From the physical setup, it turned out to be 4.4(1) cm. In order to investigate the contrast of the Talbot revivals, a two-grating setup was used (figure 2), analogous to that in Chapman *et al.* for the atom waves.[2]

Fig. 2

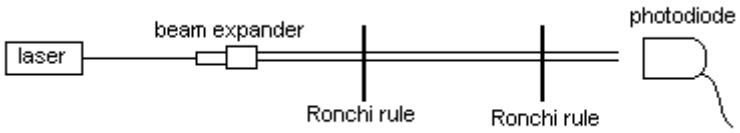

A simple photodiode measured the intensity of transmitted light, and by carefully positioning the second grating, the light at a Talbot length multiple could be either mostly blocked or mostly transmitted. This worked well out to about 6 Talbot lengths (26.4 cm), at which point the fringes of Fraunhofer diffraction started to be visible. The result can be seen in figure 3.

Fig. 3

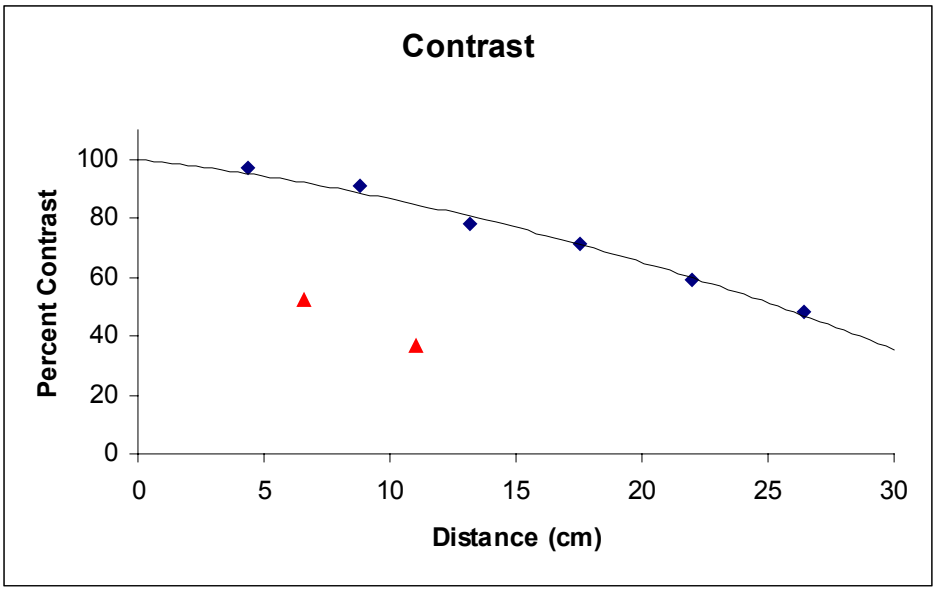

Since the contrast will always have a local maximum at integer multiples of the Talbot length, the curve that is fit to these points represents the contrast envelope, under which the real contrast structure is contained. Models predict that there is always some structure present so that contrast never goes down to zero completely, but that could not be measured in this case because of the lack of the right masks.

Replacing the second Ronchi rule with a fine one (12 lines/mm), allowed measurements of some of the half-period revivals (triangles), which are also included in the contrast graph. In between the first and second Talbot revival, the contrast of the half-period turned out to be 52%, which quickly dropped down to 37% between the next two. With the right equipment, I could have exposed film at one of these distances in order to record these patterns permanently. This would be analogous to placing a surface at a Talbot length for matter waves and depositing the corresponding structure. This demonstration of the optical Talbot effect, which is not commonly known even among physics students, illustrates the ease of the effect's accessibility and manifestation. Therefore, it should be a great candidate to take into the realm of atom optics.

THEORETICALLY SPEAKING…

In order to probe the origins of the Talbot effect, to derive the Talbot length, and to make some predictions about how the atom waves will behave under certain conditions, one must venture into the theory. The Talbot effect, just like far-field diffraction, basically stems from the fact all the waves transmitted through different windows diffract and interfere with each other. However, in the near field the curvature of the wavefronts cannot be ignored, since it has a strong effect on the resulting intensity pattern. This is commonly known as Fresnel diffraction. The relation necessary for Fresnel diffraction to occur is defined by the wavelength, the distance from the grating z, and the illuminated grating area ρ as $\rho^2 \geq \lambda z$.[12]

Fig. 4

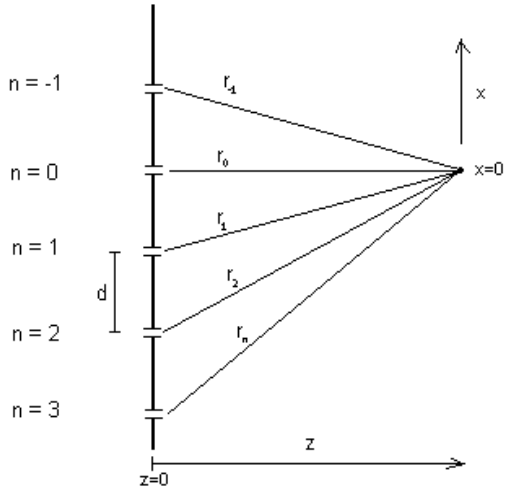

In general, we can make use of the Huygens' wavelets principle, which states that every point on a wave acts as a point source, oscillating in phase with the incident wave. Thus, the grating can be viewed as a collection of radiating point sources. In the simplest case we neglect the width of the slit, and each slit contains only one radiator. The resulting picture is shown in figure 4. For a set of infinite slits, the wavefunction at the point (r) will be described by

$$\Psi(r) = \sum_{n=-\infty}^{\infty} \frac{e^{i(kr_n - \omega t)}}{\sqrt{r_n}}$$

where r_n is the distance of the n-th slit to the point, k is the wavenumber, and ω the angular frequency. The $r^{-1/2}$ dependence comes from the fact that the intensity must decrease as $1/r$ for cylindrical waves in order to conserve the total probability. Since intensity or atom flux is the measurable property, we have to find the square of the wavefunction averaged over time. This becomes

$$\left\langle I(r)\right\rangle_t = \left\langle \left| Ne^{-i\omega t}\sum_n \left[\frac{\cos(kr_n)}{\sqrt{r_n}} + \frac{i\sin(kr_n)}{\sqrt{r_n}}\right]\right|^2 \right\rangle_t$$

$$I(r) = \left|\sum_{n=-\infty}^{\infty} \frac{\cos\left(\frac{2\pi}{\lambda}\sqrt{z^2+(x+nd)^2}\right)}{\sqrt{r_n}}\right|^2 + \left|\sum_{n=-\infty}^{\infty} \frac{i\sin\left(\frac{2\pi}{\lambda}\sqrt{z^2+(x+nd)^2}\right)}{\sqrt{r_n}}\right|^2$$

To find the z coordinate of a revival, we can solve for the value of z (at x=0) that causes a maximum of intensity. This will occur when the first term equals 1 for all n. Neglecting the $r^{-1/2}$ for now, it means that the argument of the cosine must be a multiple of π, i.e. for any n there exists an integer m such that

$$\frac{2\pi}{\lambda}\sqrt{z^2+(nd)^2} = \pi m$$

Expanding this to first order in $(nd/z)^2$,

$$\frac{2z}{\lambda}\left(1+\frac{1}{2}\left(\frac{nd}{z}\right)^2 - O\left(\frac{nd}{z}\right)^4 + \ldots\right) = m$$

and subtracting $2z/\lambda = m_0$, we get a formula for the Talbot revivals.

$$z = \frac{n^2}{m}\frac{d^2}{\lambda}$$

Since there exists for all n an integer m that satisfies this equation, it means that every slit contributes in phase at the position $z = d^2/\lambda$. In order to neglect terms of order $(nd/z)^4$ and higher, as was done in the expansion, the relation that must be satisfied is

$$\frac{2\pi z}{\lambda}\frac{3}{8}\left(\frac{nd}{z}\right)^4 << \pi$$

which leads to the relation that $n^2 < d/\lambda$. As long as this condition holds, the approximation should be valid. On a more physical note, the said approximation is just like taking the wavefront to be parabolic instead of spherical. For the proposed experiment as well as the simulations presented in this thesis, the grating period was 100 nm and the atom wavelength ($\lambda = h/p$) was 0.01 nm. Hence the number of contributing slits must be less than 100 for the parabolic wavefront approximation to hold. In order to neglect $r^{-1/2}$, we must check that it does not contribute much past the distance of one Talbot length, since that is the region we are most interested in. Indeed, for the number of illuminated grating bars and the Talbot distance, the $r^{-1/2}$ contributes a factor of only 10^{-4}.

NOT QUITE PERSIAN, BUT PRETTY NONETHELESS

We can apply this basic theory in computer models to try to simulate the Talbot carpet (see Appendix A). In order to account for the finite size of the windows, the Huygens' wavelets principle has to be taken one step further. Now the width of the window must be approximated as a collection of wavelet sources. All of the following simulations are calculated with a 100 nm grating period, but the slit width is one of the varying parameters. The first Talbot carpet pattern comes from a grating model with 10 nm windows, corresponding to a 10% open fraction. Each window was represented by 10 individual sources spaced 1 nm apart, and a total of forty windows were used to calculate the patterns. This proved to be plenty to approximate the resulting carpet, but stayed well under the limit imposed by the parabolic approximation. Although the slit width was changed, the density of one wavelet per nanometer and the sum over forty slits were also kept constant for all the models. Increasing these parameters did not cause noticeable change in the resulting intensity distribution. The atomic wavelength initially used in the calculations is 0.01 nm. This, by way of the deBroglie relation describing atom waves, corresponds to sodium atoms traveling at about 1000 meters per second. Thus, according to the formula for Talbot length, the first revival appears at one millimeter.

Fig. 5

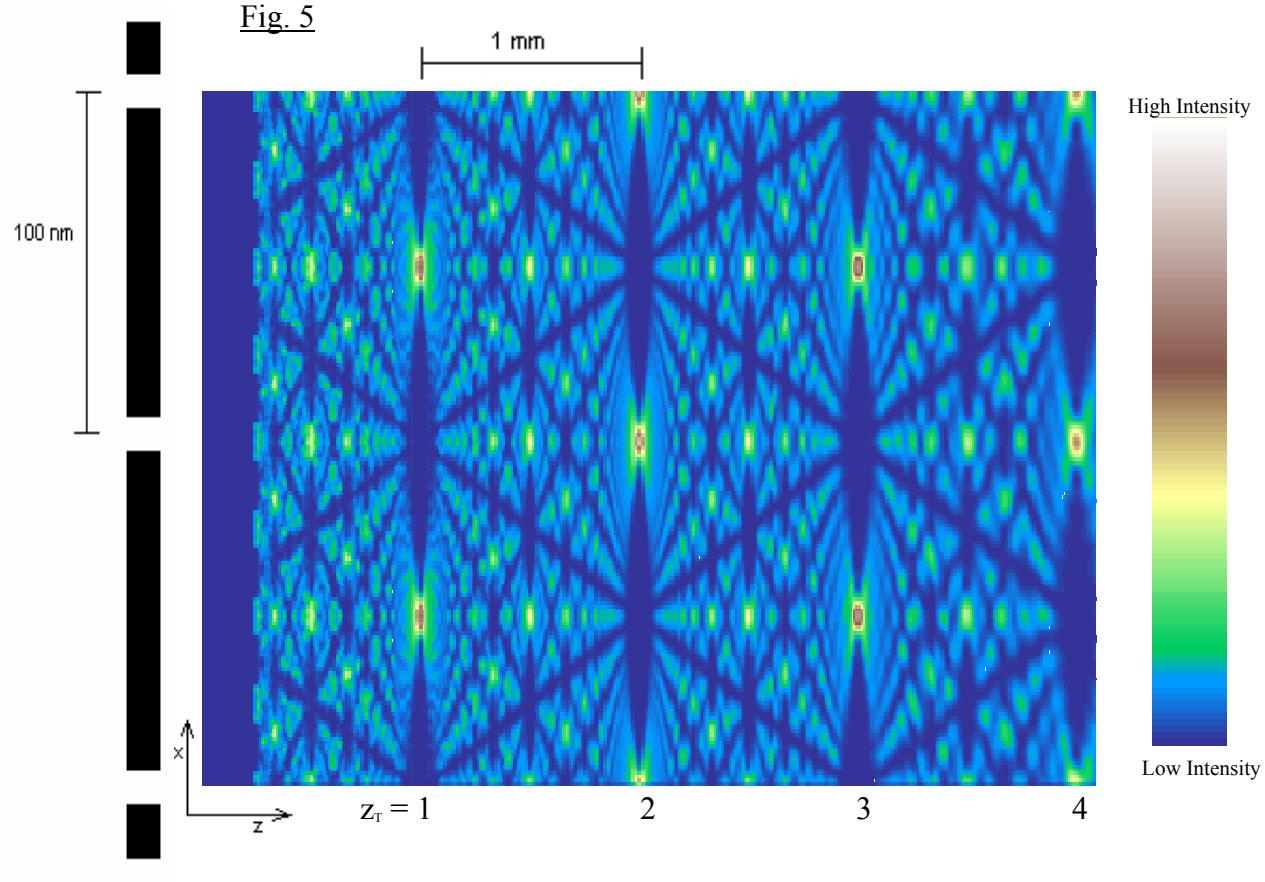

Figure 5 exhibits the pattern produced by 10 nm windows. The pattern on the left shows the location of the windows, and the bottom axis corresponds to z measured in Talbot lengths. It is important to note a clarification of convention here. The pattern clearly shows the full period revivals, but they are shifted by half a period for every revival. Some define the Talbot length as $z_T = 2a^2/\lambda$, and state that there is a full period revival with a half-period shift at 0.5 and again at 1.5 Talbot lengths. These conventions are of course equivalent, but I will continue to use the one as previously defined and illustrated in figure 5. It is also important to keep in mind that the axes have two very different scales. While the bottom axis is about four millimeters long, the left axis spans 200 nm, meaning the bottom would be stretched to about 20,000 times its current length in order to be proportional. The half-period revivals also show up nicely in this model at $z = z_T\,(n + ½)$, as well as the thirds of a period at $z \approx 2z_T/3$ and again at $z \approx 4z_T/3$. It is no

coincidence that the well-defined areas of the carpet are reminiscent of fractals. Berry *et al* explains in a PhysicsWeb article that there are an infinite number of images at fractional distances of the Talbot distance. However, at irrational fractions of this distance, such as $z_T/\sqrt{2}$, the intensity as a function of the grating coordinate is actually a fractal function, continuous but not differentiable .[13]

Expanding the windows to a 30 nm size changes the Talbot carpet dramatically. Figure 6 illustrates this nicely. The main revivals are still clearly visible, yet they have started to form interesting "lobes" on either side, at z slightly greater and less than z_T.

Fig. 6

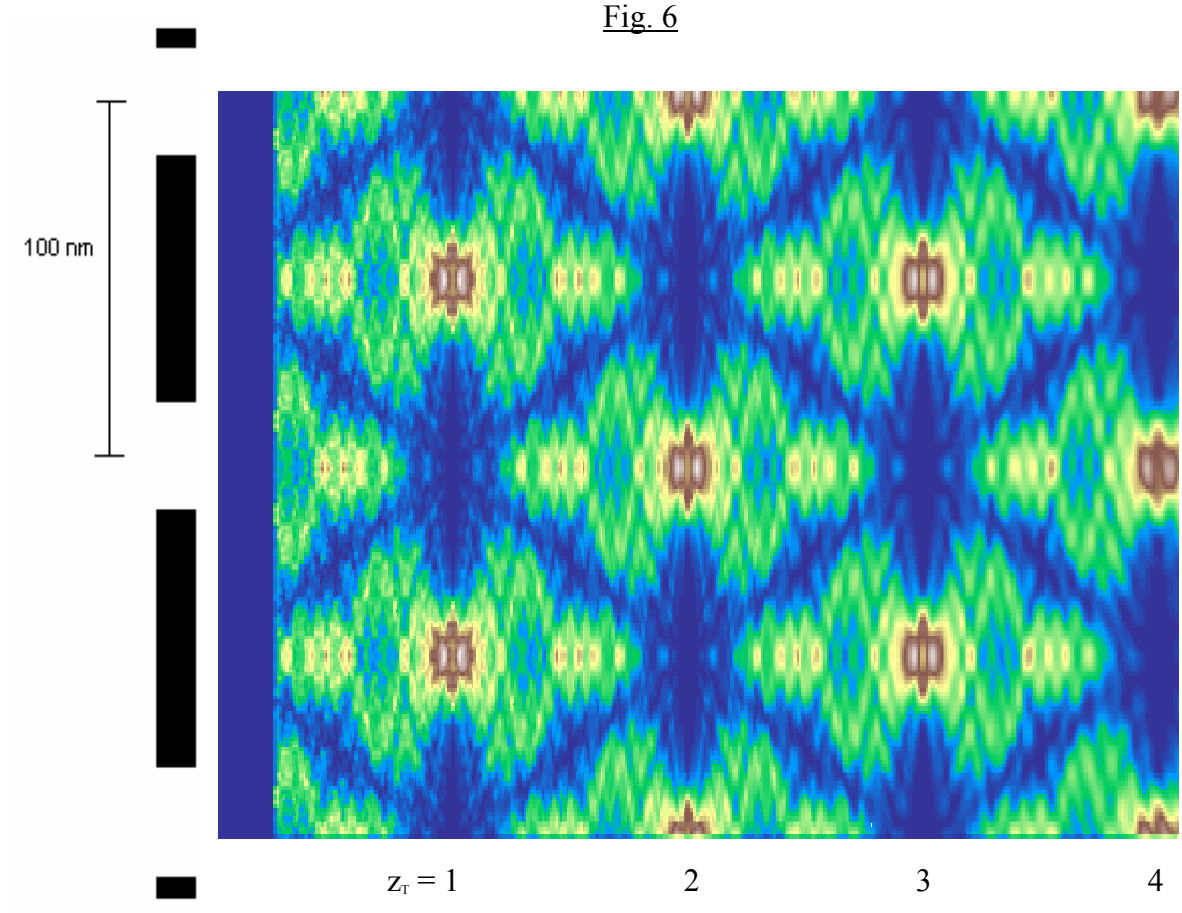

The revivals are very well defined, but in order to see the contrast better, it is necessary to take sections of this surface and view them independently. Figures 7 and 8 are sections of this plot at one Talbot length and 1.5 Talbot lengths, respectively.

Fig. 7

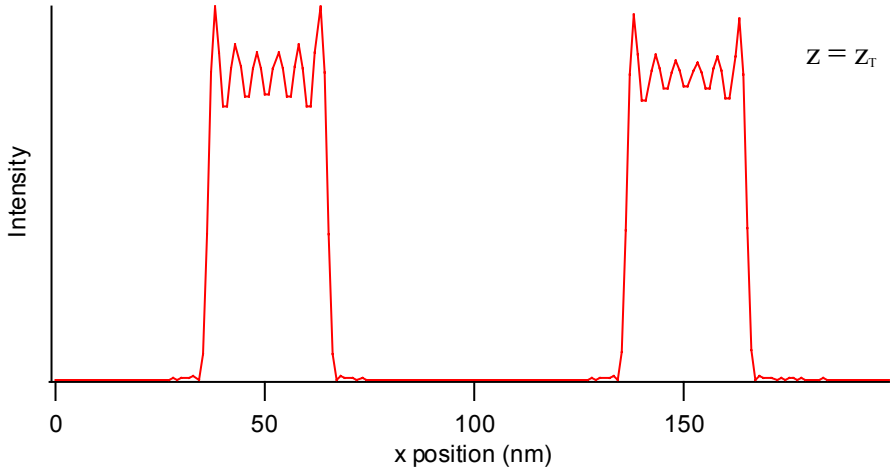

Fig. 8

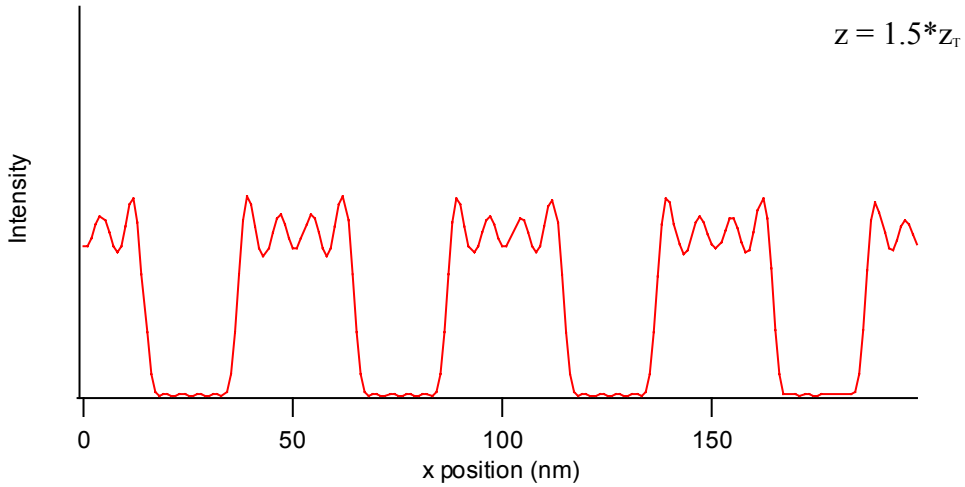

Although the absolute intensity is arbitrary, the scale as been preserved. It is clear from these two graphs that the contrast is practically 100%. The wavy structure on the tops of these "pillars" is still a bit of a mystery but might be a true diffractive effect. Window sampling density is not the cause of the fine features, since increasing the number of sources per window by a factor of 100 has no effect on it. However, the averaging effect of imperfect collimation will smooth out these features. Note that in this case, the half

period revivals have roughly the same width as the full revival. This results in a doubling of the "open fraction."

Of course, the next question is what the actual open fraction of such nanofabricated gratings might be. A Scanning Electron Microscope revealed that the gratings from the atom interferometry lab have an open fraction of about 70%. The Talbot carpet with this open fraction is depicted in figure 9. Probably the most pronounced features of this carpet are the bright lobes seen to either side of the full revival at z slightly greater or less than nz_T. Once again, it is helpful to take cross sections of this graph and view them separately (figs. 10, 11, 12).

Fig. 9

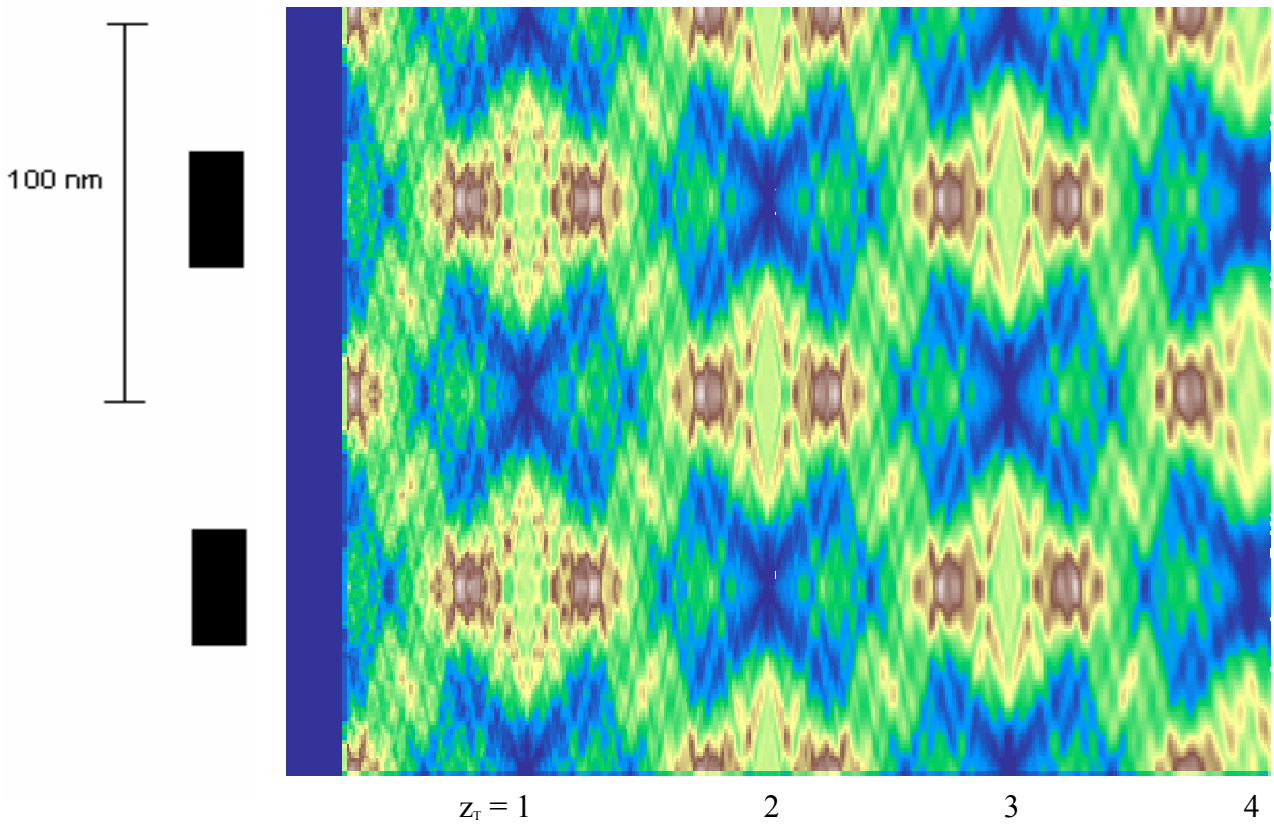

The full period revivals at $z = nz_T$ are about as expected: 70 nm long plateaus with some squiggles on top. However, the half period revivals at $(n + ½)\, z_T$ have very different characteristics than in the previous case: Their absolute intensity is equal to that of the full revival, yet they are only about 20 nm wide. Also, since the intensity never goes down to zero, there is quite a loss in contrast, down to about 30%. The contrast is defined to be the difference of maximum and minimum intensities divided by their sum,

$$contrast = \frac{I_{max} - I_{min}}{I_{max} + I_{min}}$$

When taking a cross section through the peak of one of the lobes, at about $(n \pm ¼)\, z_T$, one gets the by far the highest intensity and sharpness. If this is can be observed in the lab, it might be useful to take advantage of this focusing effect when the exact shape of the structure is not that important.

Fig. 10

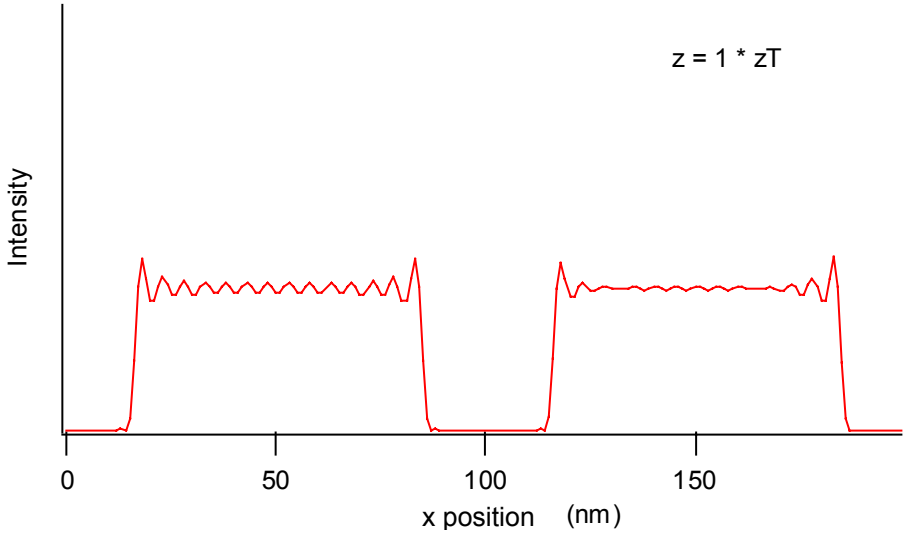

Fig. 11

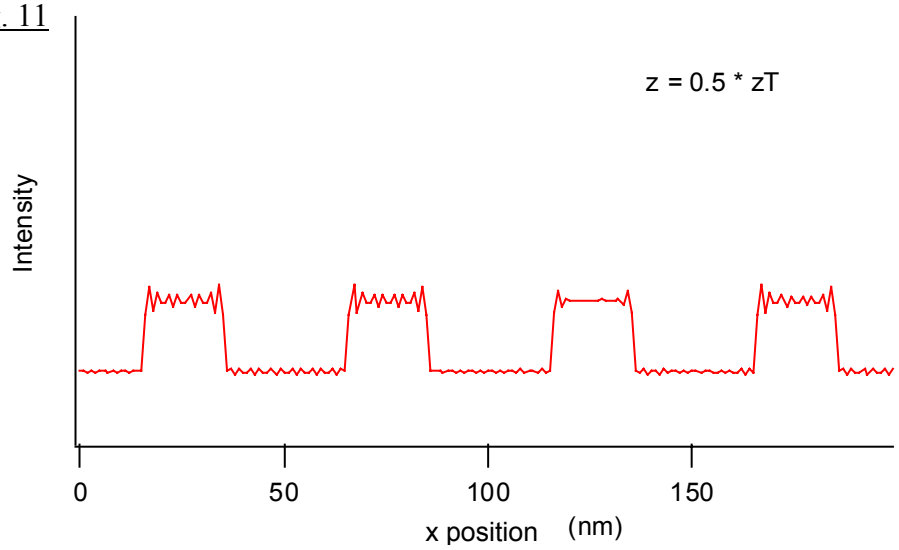
z = 0.5 * zT
Intensity
0
50
100
150
x position (nm)

Fig. 12

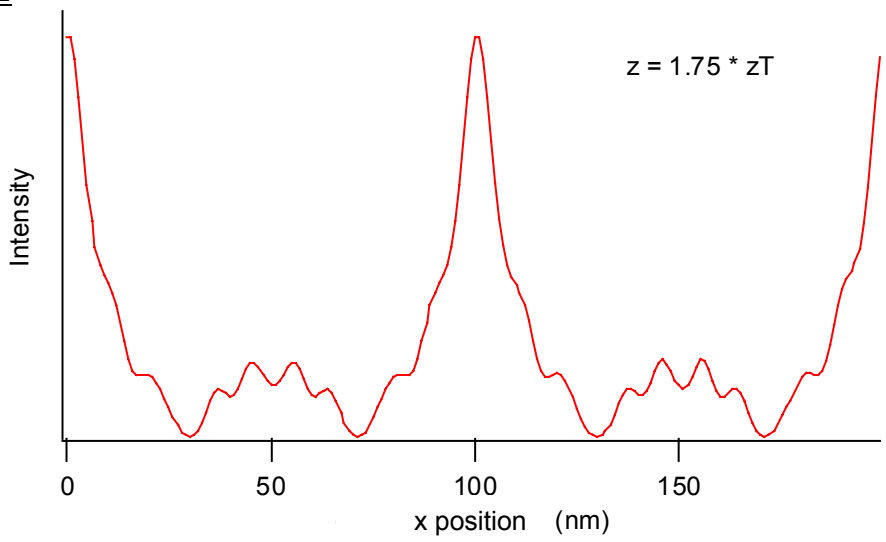
z = 1.75 * zT
Intensity
0
50
100
150
x position (nm)

These models bring up another question. How far behind the grating will the revival pattern persist, and how quickly does the contrast decrease? By taking the last simulation, and going out to 30 Talbot lengths (fig. 13), one can see that the finer patterns disappear by about 10 times the Talbot distance, or about 1cm. After about another centimeter (10*z_T), even the roughly periodic structure begins to die out. Amazingly enough, there is still 95% contrast out at 15 times the Talbot length. After that, the contrast slowly drops to 70% at 20 zT, and then quickly to 25% at 25 zT. After that all of the structure basically washes out, except for the Fraunhofer diffraction that will start to emerge.

One test to show that the Talbot carpet model is working properly would be to verify that the same model

Fig. 13

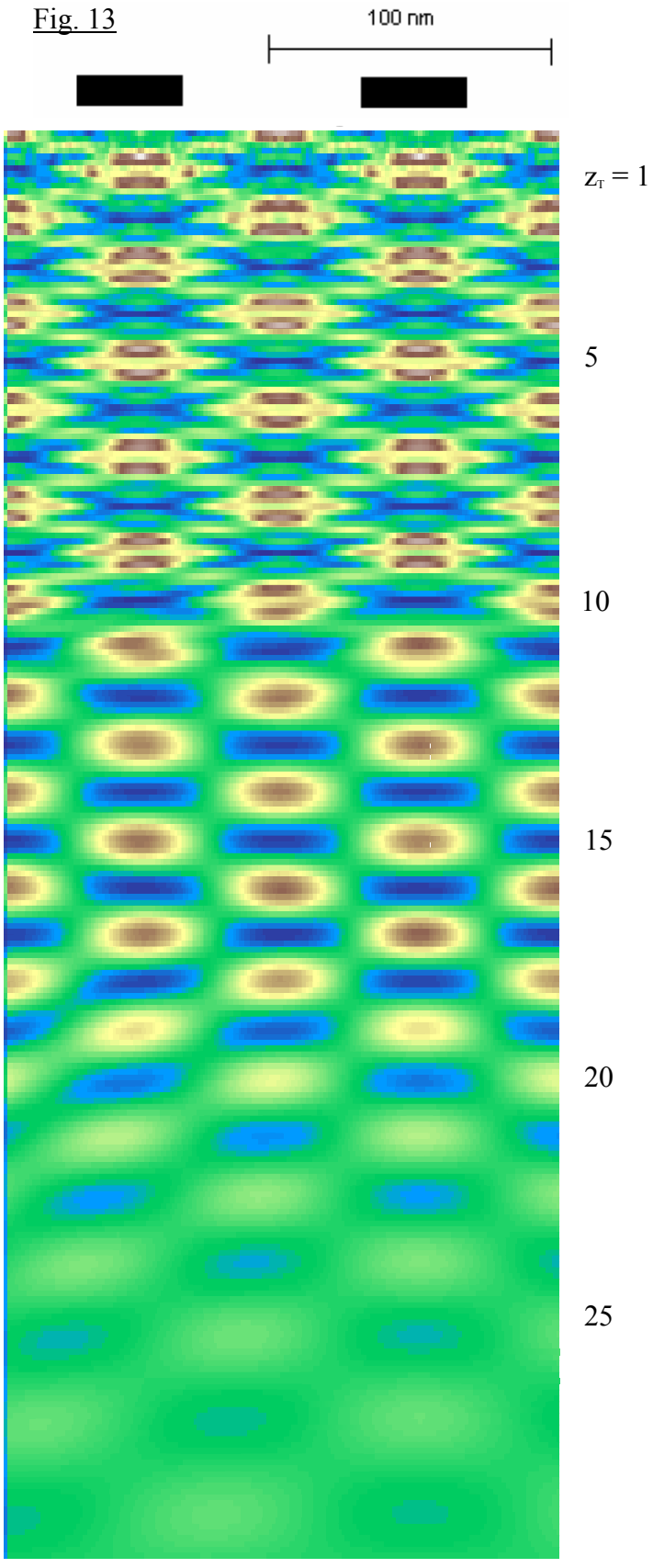

predicts the diffraction pattern in the far field. Unfortunately, this is only somewhat the case. I tried the same parameters as the optical setup that I had used, so that I had something simple to compare it to. Since the laser spot was about half a centimeter in diameter, it illuminated around 30 grating bars. The pattern in the near field did recreate the physical situation (fig. 14) in the first 20 cm behind the grating. The contrast of the full and half period Talbot revivals consistently stays at nearly 100% past $6*z_T$, unlike the measured results in figure 1. This suggests that the loss in contrast in the physical setup was due to deviations from the ideal model, such as imperfect collimation of the laser light and/or imperfections in either grating.

At a distance of 2 meters, where Fraunhofer diffraction has taken over and become very visible (since $z >> z_T$ and x >> spot size), the more familiar far-field diffraction pattern also appeared. Figure 15 shows the far-field intensity distribution, which compares well with the expected distribution. The far-field diffraction orders should peak when $\sin\theta_n = n\lambda/d$, which in this case occurs at $x = n*$ 7.7 mm and matches the model. The envelope of the diffraction orders should be given by $[\sin(\theta w/\lambda)/(\theta w/\lambda)]^2$ and is shown with a dashed line in figure 15. Because of the 50% open fraction, the minima from single-slit diffraction occur at exactly twice that distance, which explains the missing orders at $n = \pm 2, \pm 4$, etc. The jagged peaks would effectively be smoothed out with imperfect beam collimation, since the distribution will be slightly displaced in x for a beam coming in at an angle.

Fig. 14

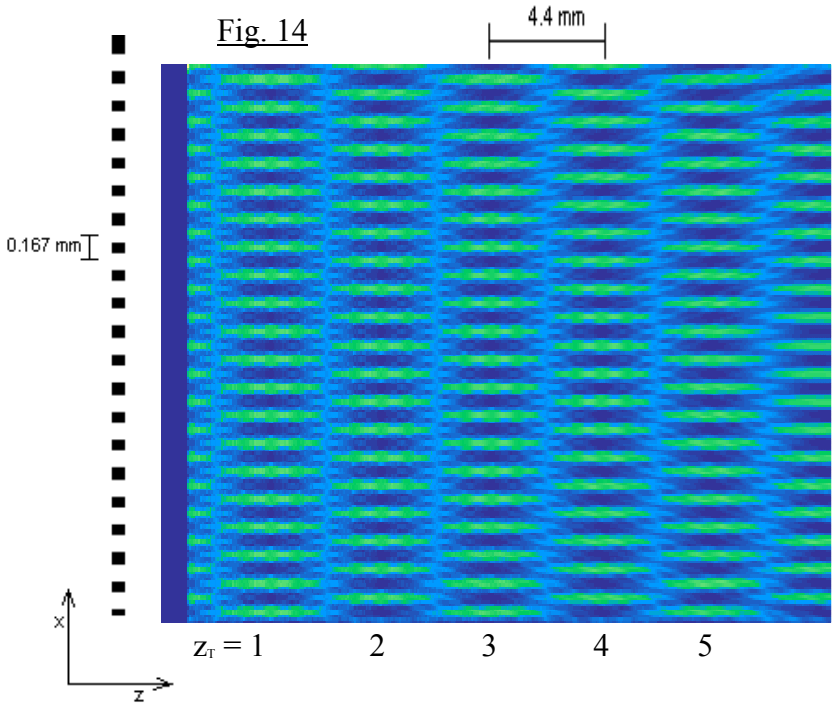
4.4 mm
0.167 mm
x
z
z_T = 1
2
3
4
5

Fig. 15

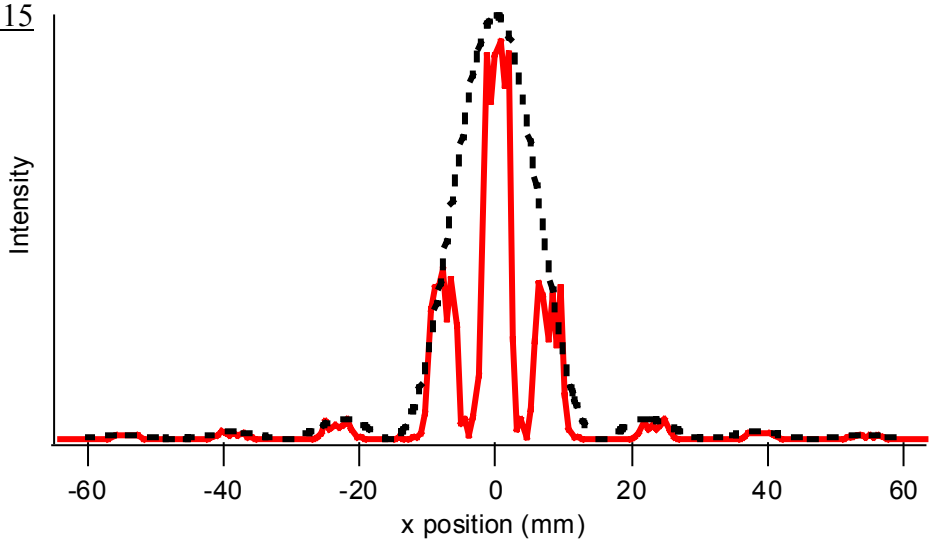
Intensity
-60
-40
-20
0
20
40
60
x position (mm)

VAN DER WHO?

Up until this point, the models might as well have been describing any waves, since no part of the models other than the wavelength were specific to matter waves. However, unlike optical waves, matter waves passing through the slots of a grating will actually be affected by the walls a finite distance away. This interaction is called the van der Waals force, and stems from the ability of neutral atoms to become polarized and attract each other. For two free atoms in vacuum, this force has a $1/r^6$ dependence. For the interaction between an atom and a plate, which is the more nearly the case for the gratings, this force goes as $1/r^3$. In terms of matter waves, one can think of it as a potential that they pass through. This potential will introduce a phase shift (fig. 16). Assuming that the wavefunction is given by

$$\psi = e^{ikz-\omega t}$$

then the time-independent Schrödinger equation is

$$-\frac{\hbar^2\nabla^2}{2m}\psi = (E-V)\psi$$

yielding

$$k = \sqrt{\frac{2m}{\hbar}(E-V)}$$

$$k_0 = \sqrt{\frac{2m}{\hbar}E} \quad \text{and} \quad \varphi_0 = k_0 z$$

Now we want the phase shift given by

$$\Delta\varphi = \varphi - \varphi_0 = (k-k_0)z$$

If we now take $z = t$ and $V = -C_3/r^3$, then we get

$$\Delta\varphi = \sqrt{\frac{2m}{\hbar^2}}\left[\sqrt{E} - \sqrt{E + \frac{C_3}{r^3}}\right]t$$

$$\Delta\varphi = \frac{-\sqrt{2m}}{\hbar}\frac{1}{\sqrt{E}}\frac{C_3}{r^3}\frac{1}{2}t$$

Using the energy relation $E = \frac{1}{2}\, mv^2$ in the above equation, we get

$$\Delta\varphi = \frac{-C_3 t}{\hbar v r^3}$$

Finally, applying the fact that the atom will feel the potential from both sides, the phase shift is given by

$$\Delta\varphi = \frac{tC_3}{\hbar v}\left[abs\left(\xi - \frac{w}{2}\right)^{-3} + abs\left(\xi + \frac{w}{2}\right)^{-3}\right]$$

Here t is the thickness of the grating (in the same direction as the atoms are traveling), w is the slit width, v is the velocity of the atoms, ξ is the grating coordinate, and C_3 is a coefficient that depends on the specific substances involved.[14]

Fig. 16

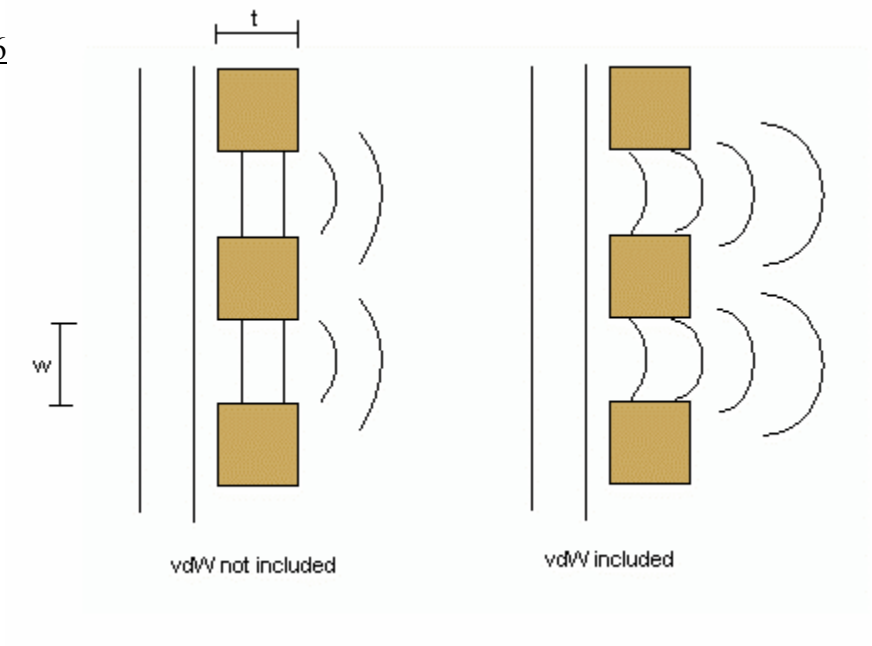

In order to account for the van der Waals force, I simply added the position-dependent phase shift as given above to the phase of the Huygens' wavelet in the simulations (see Appendix A). Using C_3=5 meV nm^3 as expected from theory, I combined all the constants in front into one free parameter, which I will refer to as the vdW phase coefficient, and which comes out to be somewhere around the order of 0.5 nm^3. Thus the vdW phase difference is given by $0.5/r^3$ where r is the distance to the grating wall in nm.[14]

It turns out that the vdW forces do not strongly affect the intensity distribution. Figure 17 shows two close-ups of a full-period revival at one Talbot length from the grating. The one on the left does not take the interaction into account at all, and the right one was calculated with a vdW coefficient of 100 nm^3, corresponding to C_3 = 2000 meV nm^3! A value closer to the calculated value of 0.5 nm^3 makes the two almost indistinguishable. Figure 18 shows cross-sections of the two plots at $z = z_T$ and $z = 1.5\ z_T$.

Fig. 17

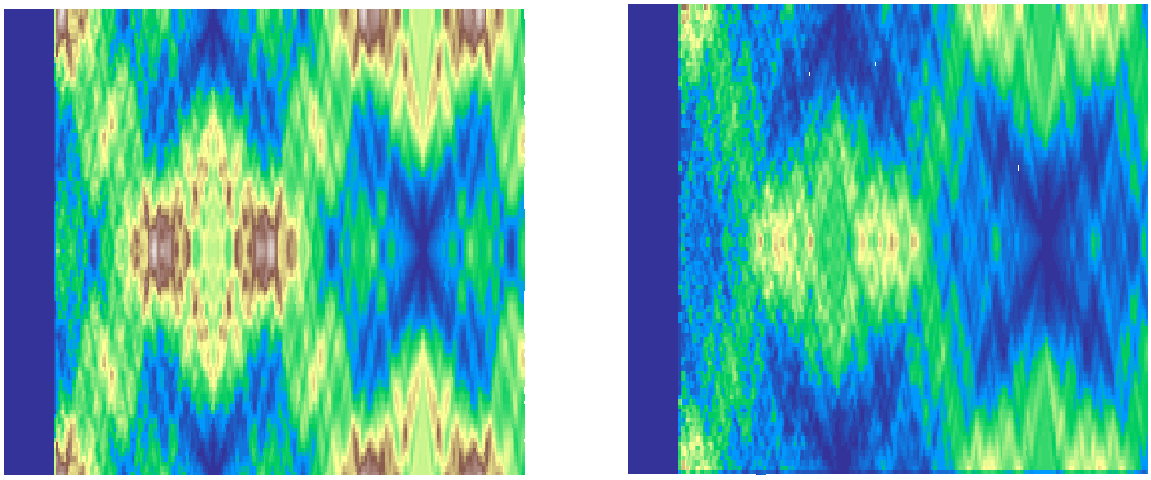

$C_3 = 0$ $C_3 = 2000$

Fig. 18

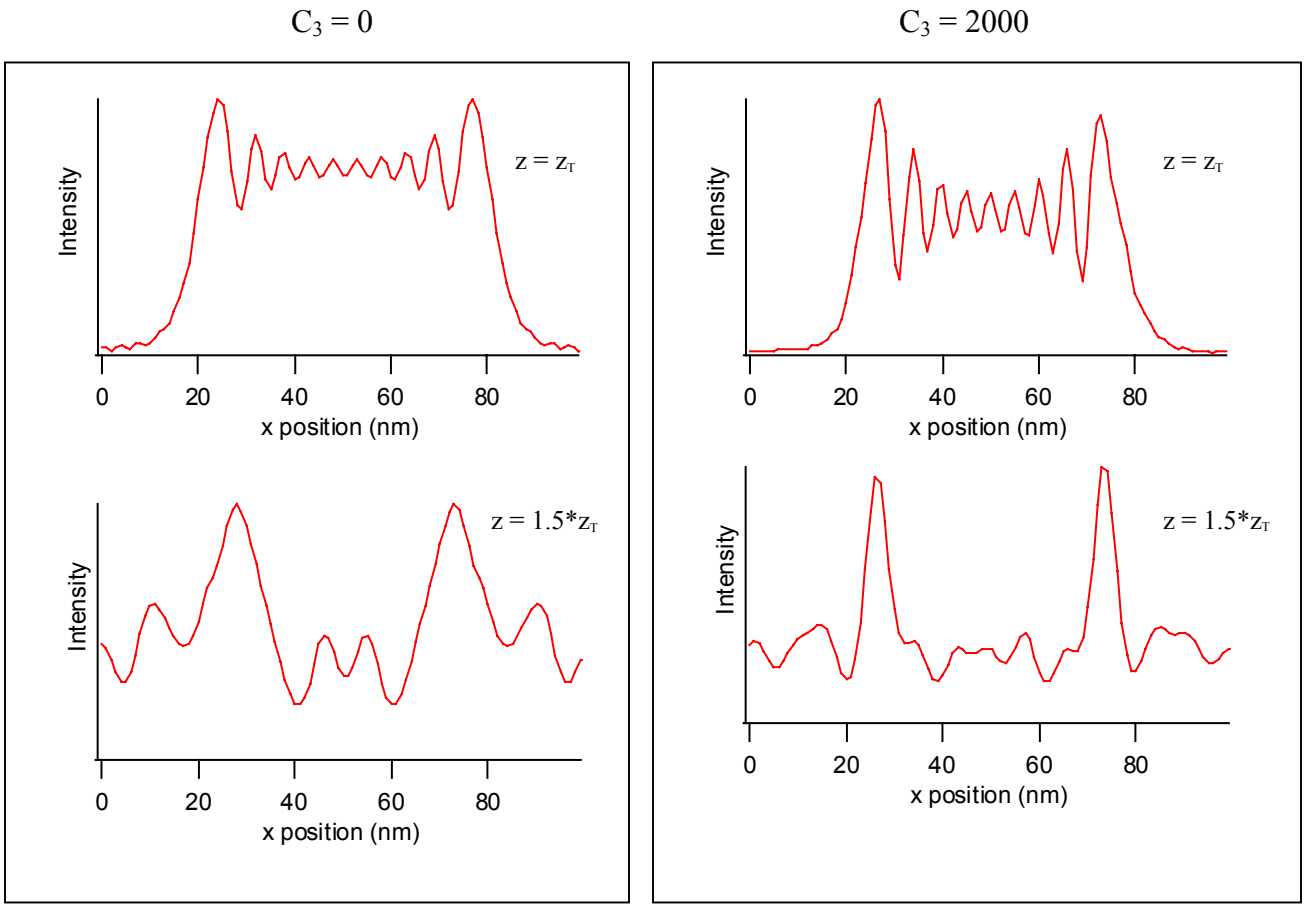

By looking further down the beam and analyzing the effect of the vdW interaction there, one can see that it is not very strong in that region either. Since these pictures take up quite a bit of space, I have added them in Appendix B. The effect of the van der Waals force in the far field is currently a hot topic of study in Dr. Alex Cronin's lab, since these forces are notoriously difficult to measure.

VELOCITY SPREAD

Another imperfection to include in the simulation is the fact that an atom beam does not have a single wavelength. Although atom lasers are beginning to become a reality, they are not yet readily available. Until then, an atom beams with various velocity distributions must be used. The velocity spread of an effusive beam can be narrowed greatly through the use of supersonic expansion. To calculate the Talbot carpets generated with a spread in velocities, I assumed a Gaussian distribution and used its sigma as a parameter. This assumption roughly approximates the continuum of beams, from effusive with $\sigma = \langle v \rangle/2$ to supersonic with $\sigma = \langle v \rangle/20$. Each velocity translates into a different wavelength, creating many distinct interference patterns. These were weighted by the velocity's probability according to the Gaussian and the resulting intensities summed together.

A thermal beam with a carrier gas has been shown to achieve a spread of velocities 5-10% of the average velocity, so I used 10% as my lower limit.[14] A thermal beam, which follows Maxwell's velocity distribution[15]

$$P(v) \propto v^3 \exp\left(\frac{-Mv^2}{2kT}\right)$$

has a rather large spread, which is why I used 50% as my upper limit. Since such a distribution generally tends to blur things out, it is expected that the finer features of the Talbot carpet disappear first. This is visible in a detail of the first full period revival in the left side of figure 19. The average velocity in this model is 1500 m/s, and the sigma here is the lower limit, 150 m/s. The full and first half-period revivals are still visible

here, as are the prominent lobes. Taking sections of these two areas reveals the shape and contrast (fig 20). The contrast for the full period revival lies at 81%, whereas that of the half-period revival is at only 34%. The effect of a velocity distribution that has a spread half as large as the average velocity can be seen in the right side of figure 19. Any and all structure completely disappears, making the purely thermal beam ineffective to observe the Talbot effect.

Figure 19 brings up two questions: Why is the grating structure not visible at small z, and why can the Talbot effect be observed optically with a regular incandescent light bulb? To answer the first question, one must remember that the model made the assumption that the contribution of the $1/r_n$ term is negligible. This does not hold very close to the grating, and wavelets from the other windows will contribute much too strongly, thereby washing out the grating structure. The second discrepancy stems from the fact that the model shows merely intensities, with no reference to the wavelength distribution. However, since our eyes can tell the difference between the wavelengths of light, we will be able to see the various colors come into focus at different distances.

Fig. 19

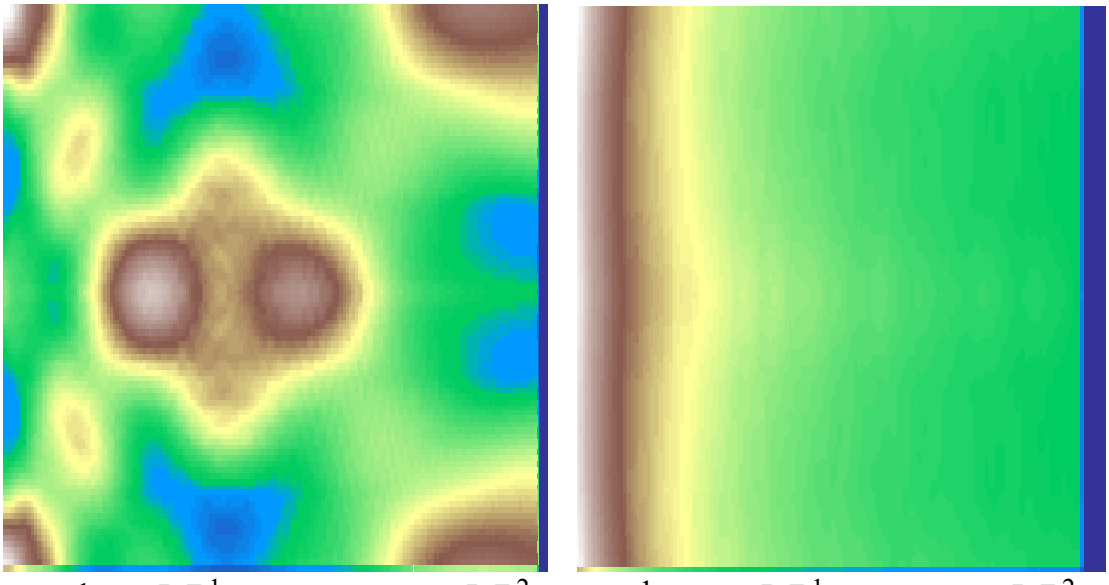

Fig. 20

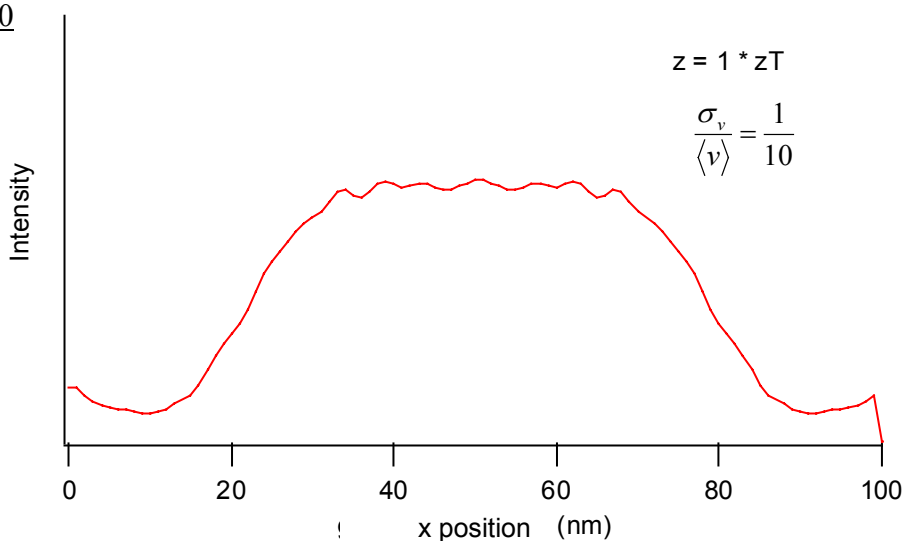

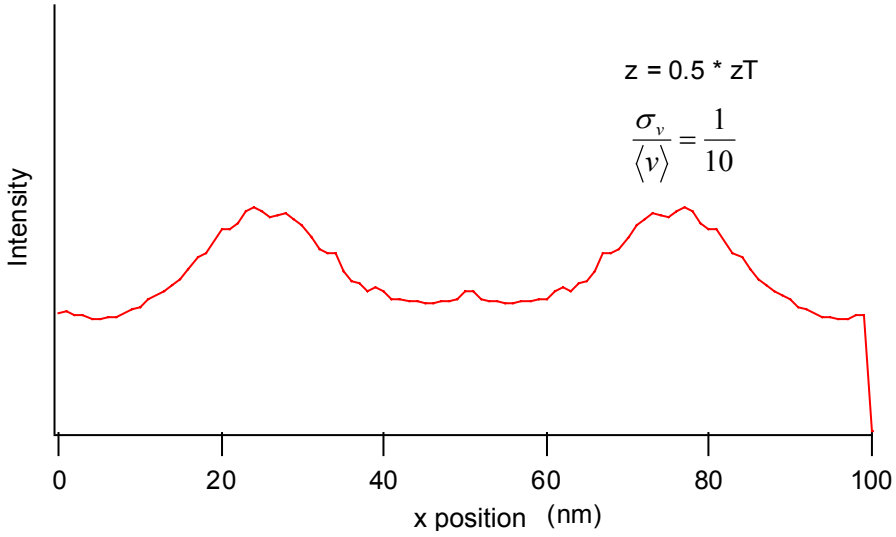

But what happens in between these two extremes, and what sort of contrast difference can one get away with? To answer that question, I put together six surface plots, all going out to 8 times the Talbot length in figure 21. The sigma value ranges from 0 to 650 with an average velocity of 1500 m/s.

Fig. 21

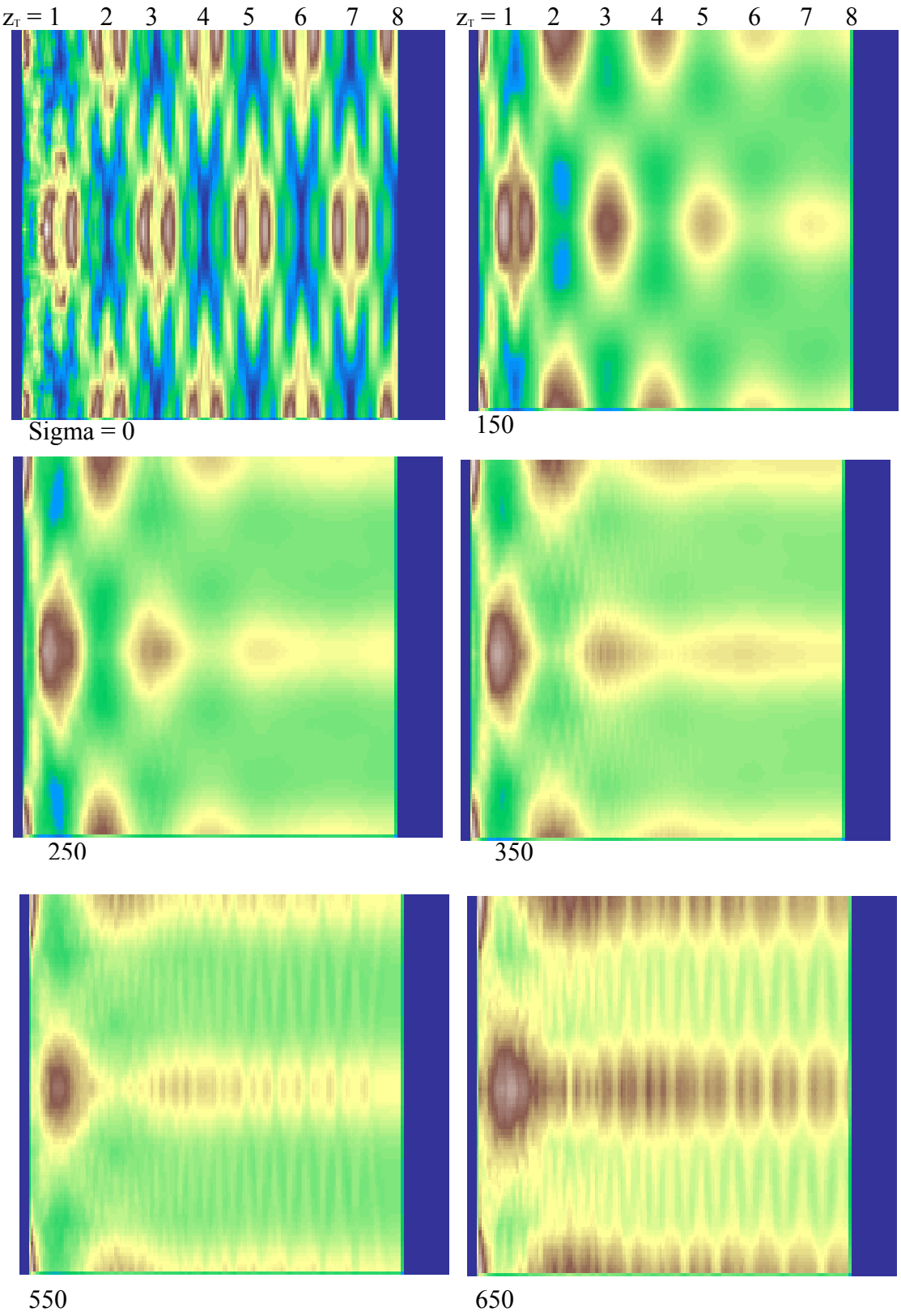

The smaller structures in the sigma = 550 and 650 plots are merely artifacts of the simulation, and disappear when the velocity sampling density is increased. The contrast at each of the Talbot lengths for all the different sigma values can be seen in figure 22.

Fig. 22

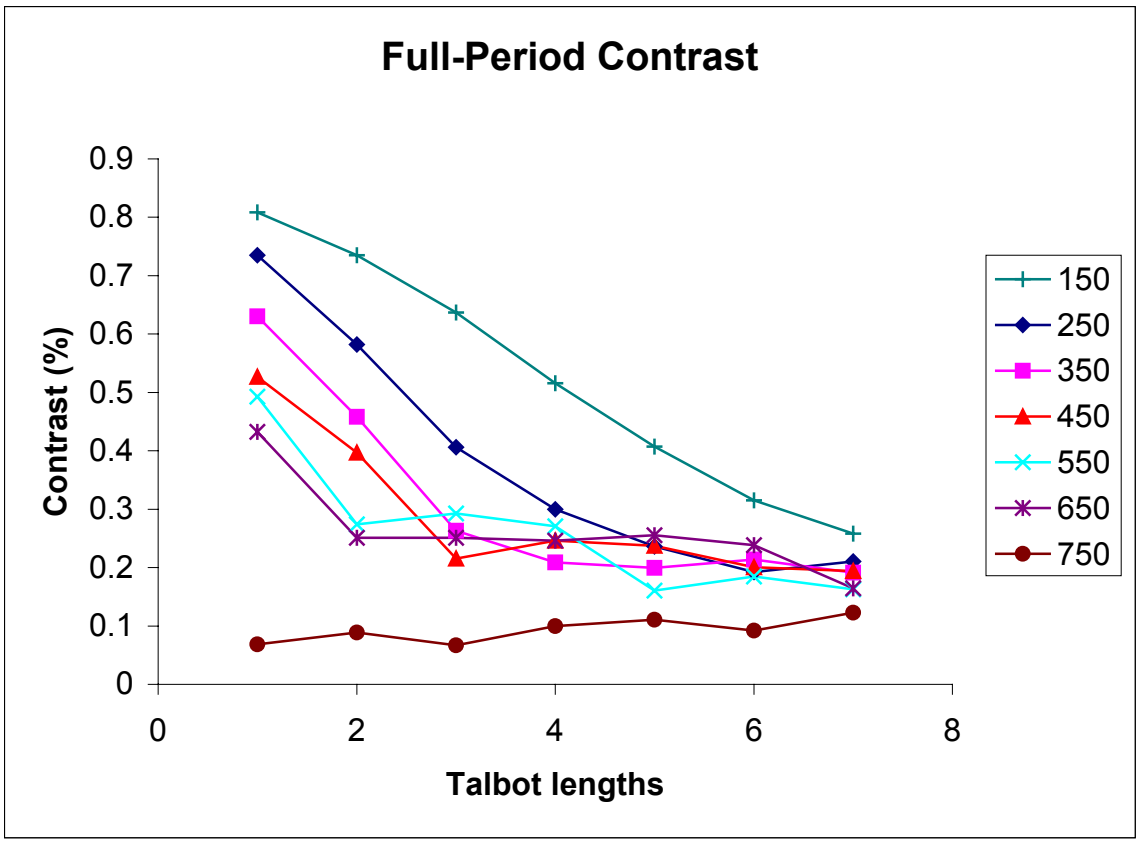

NEXT STEPS IN THEORY

To continue the analytical work, the immediate next step would be to mathematically describe fractional revivals. It would be very useful to derive expressions for their locations and to find any limiting conditions. Also, one should investigate a mathematical calculation of the contrast and predict the parameters on which it most strongly depends. Then one would need to incorporate the finite size of the windows into the equation by means of an integral. Another method of analysis that would be worth investigating both analytically and in the computer simulations is the Fourier optics method. It might prove to be more powerful, and will in any case be useful to compare its results to the results given above.

With the computer simulations there is still much to be investigated. It would be beneficial to include the $r^{-1/2}$ dependence, so that overall probability is conserved and intensities close to and far from the grating can be compared. The jagged peaks in the near and far field distribution could be an artifact of the computer simulation, or real characteristics that would manifest themselves in a perfect setup, which calls for further examination. Also, one would need to investigate the effects of imperfections in the grating bars, and how much they would affect the final distribution.

Since one of the stated advantages of Talbot assisted lithography was the possibility to use any shape, it would be worthy to investigate how true this really is. Would the fractional revivals of an arbitrary periodic shape have the same contrast as the simple grating revivals? In order to be able to compare the models to experiment better, one needs to look into the contrast plots in a more detailed manner. This would include

plotting the contrast as obtained through a second grating that is used as a mask. Another topic to go into would be the more thorough analysis of the region greater than $z = 20^* z_T$. The models showed that the revivals in that region are not quite uniform, but instead drift farther away. It would be useful to find out why. Finally, the models did not address beam collimation and its effects. Since this basically translates to a spread in incident angles, it would be similar to the velocity-spread simulations but would shift the images along the x-coordinate instead of z. Thus, a beam divergence angle of

$$\theta < \frac{d}{z_T} = 10^{-4} rad$$

is required to see the basic structures. A detailed investigation would give needed insight into beam collimation requirements, which are very useful when attempting to deposit Talbot-reconstructed images.

EXPERIMENTALISM

Although I did not get the chance to deposit atoms onto a surface using the Talbot effect, I did investigate some aspects of the necessary experimental process. In order to detect whether Talbot-assisted lithography was successful, one must have a reliable means of imaging the substrate. The structures are much too small for optical microscopes, but ideal for an atomic force microscope (AFM). The atomic force microscope uses a very small lever (about 100μm long), and pushes it cross a surface. A laser beam aimed at the lever then measures the vertical and torsional displacement, as seen in figure 23. Utilizing the AFM, I imaged a variety of nanofabricated diffraction gratings. Figure 24 shows one of these gratings in good condition. The "height" image on the left shows a 3.8 μm square scan on a vertical distance scale, where a pure white corresponds to 10 nm in height above pure black. The right image represents the exact same area, but was produced by the amount the lever twists. The three large bars are the support structures that hold the much finer grating bars.

Fig. 23

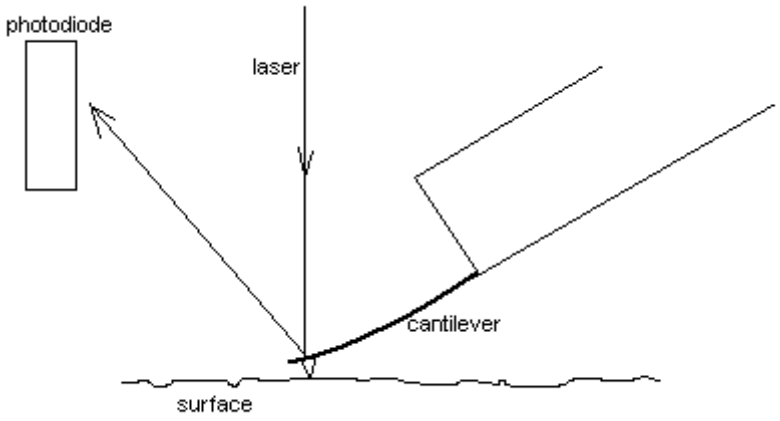

Fig. 24

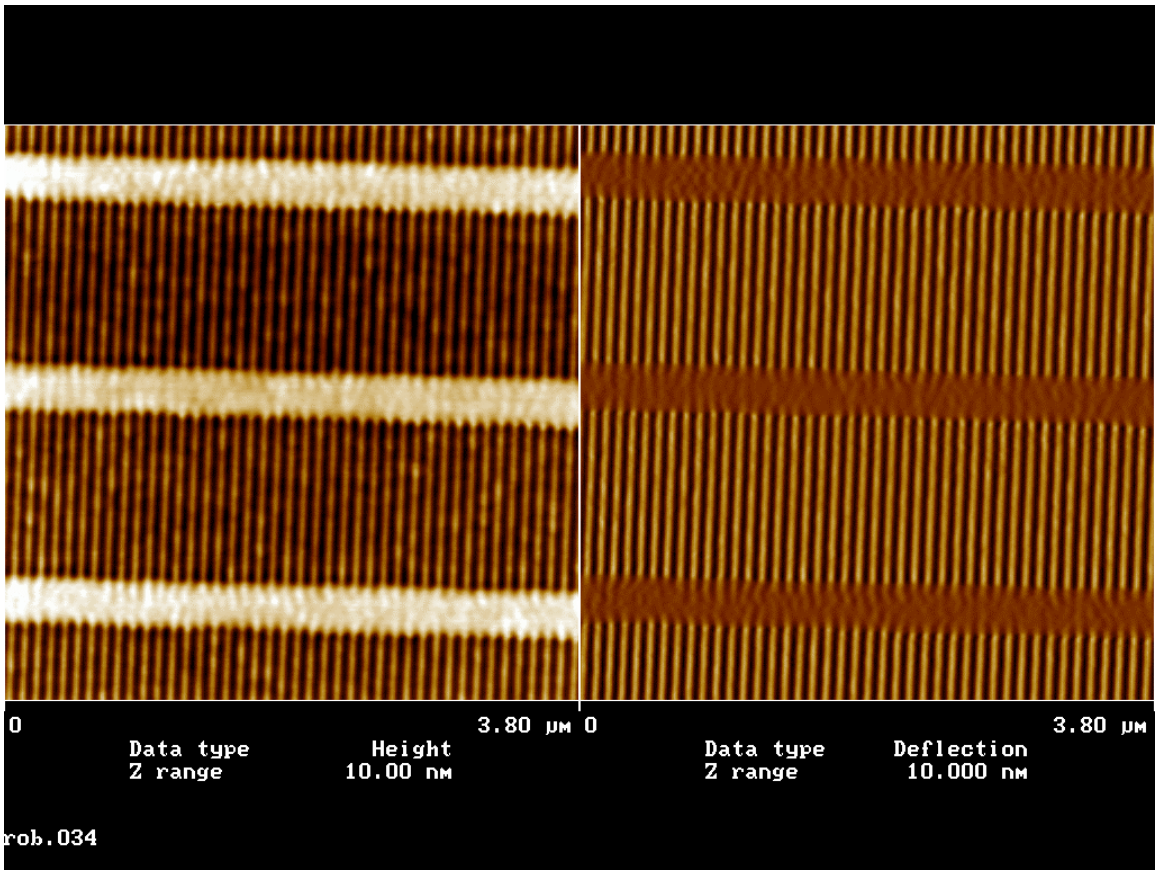
0
3.80 µm
Data type
Height
Z range
10.00 nm
0
3.80 µm
Data type
Deflection
Z range
10.000 nm
rob.034

An image of an older version of the diffraction grating is visible in figure 25. In this case, the original grating period was 200nm, as opposed to the 100 nm grating in figure 24. These grating bars were much weaker, and could not hold their original shape very well. Instead, the AFM tip moved them enough to succumb to the vdW forces between them, causing them to stick together in groups of two or three. This is an important result in that the AFM imaging can be destructive. In the case for lithography, the tip could destroy the structure if the atoms are very loosely bound to the substrate.

Fig. 25

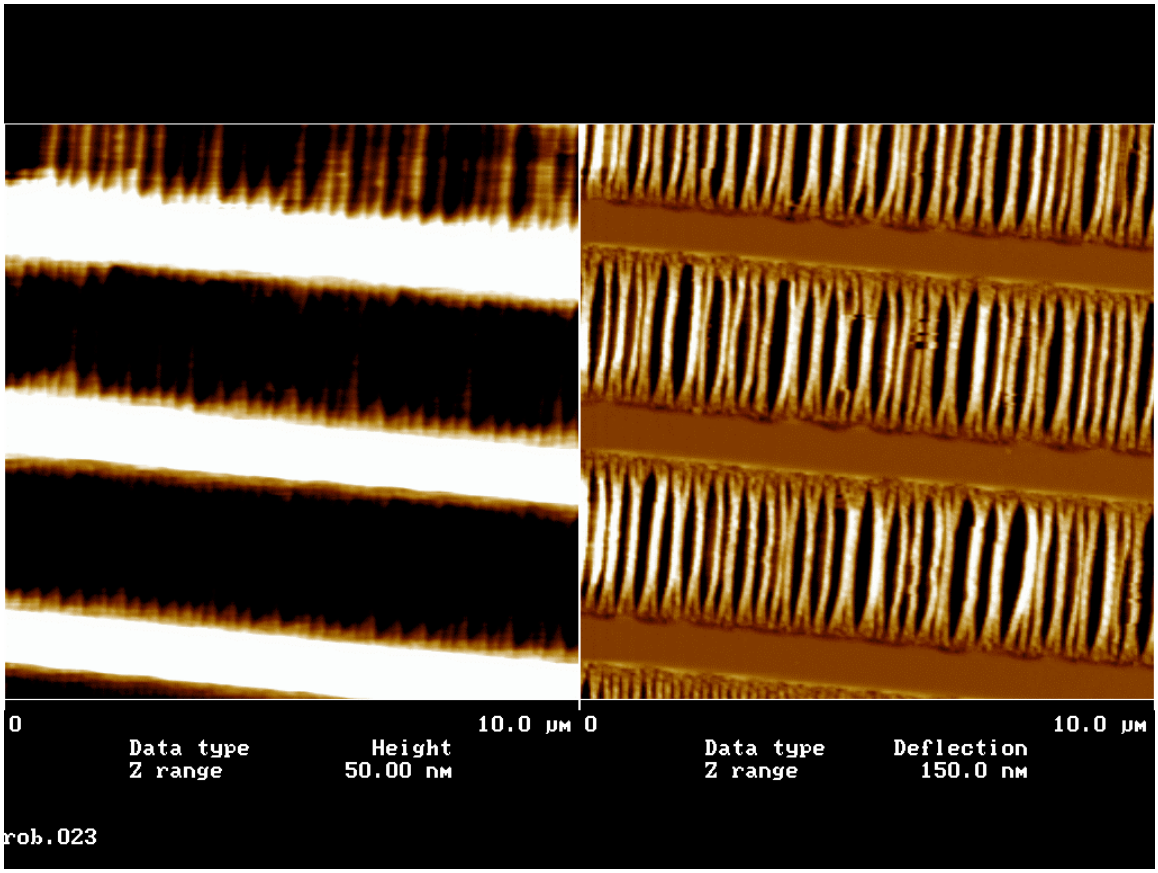

Figure 26 shows a newer grating that has been used in the sodium atom beam for a while. It is covered in easily discernible globs of sodium. This illustrates that some substances would be unsuitable for use with the Talbot effect. In this case, the sodium beam encountered the grating more or less uniformly. Since the sodium then formed clumps much larger than the grating structure, it must be relatively mobile. Thus, trying to deposit grating-sized structures of sodium on this surface (silicon nitride) would be practically hopeless.

Fig. 26

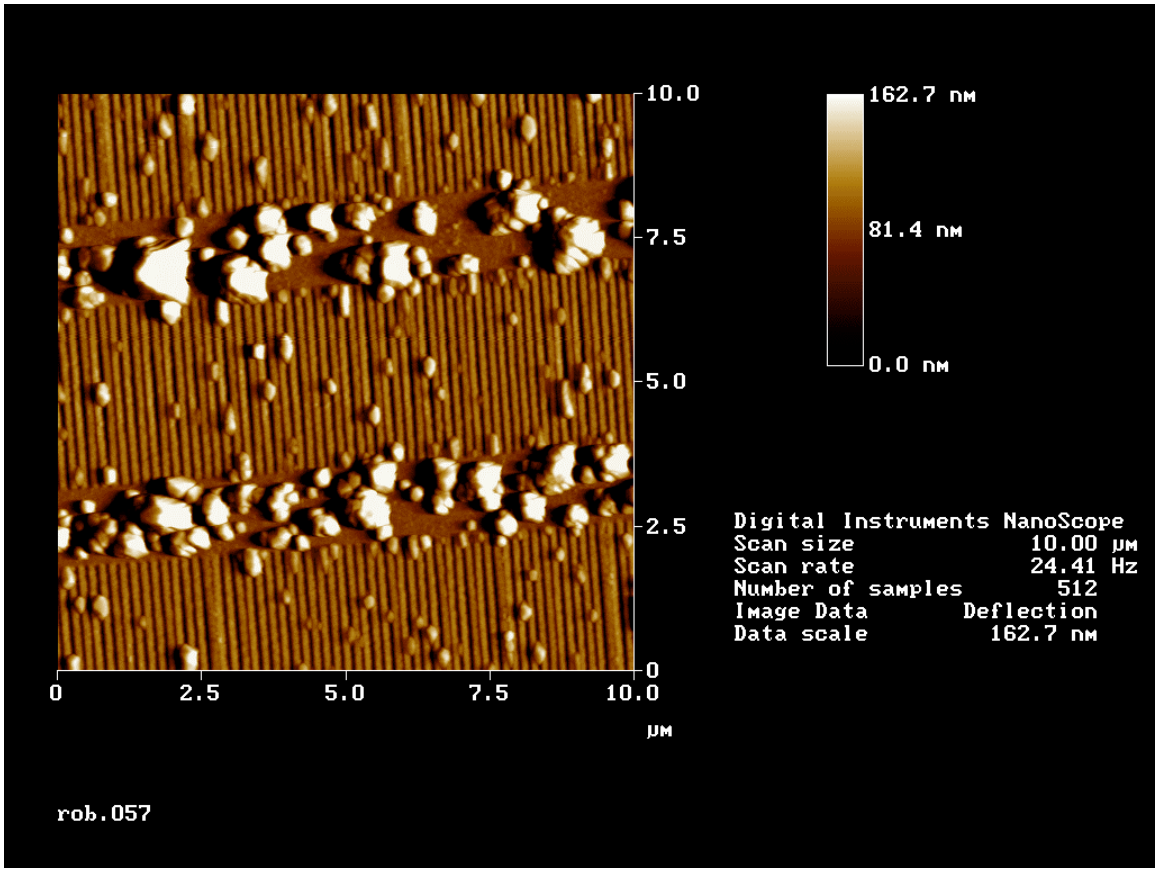

Because of the Na buildup, such gratings were thought to be only suitable for a single use. Once clogged, the gratings were retired. However, in a different research project I showed that the grating bars can be cleaned simply by immersion in water and drying in air. A picture of the same window as above after cleaning can be seen in figure 27.

Fig. 27

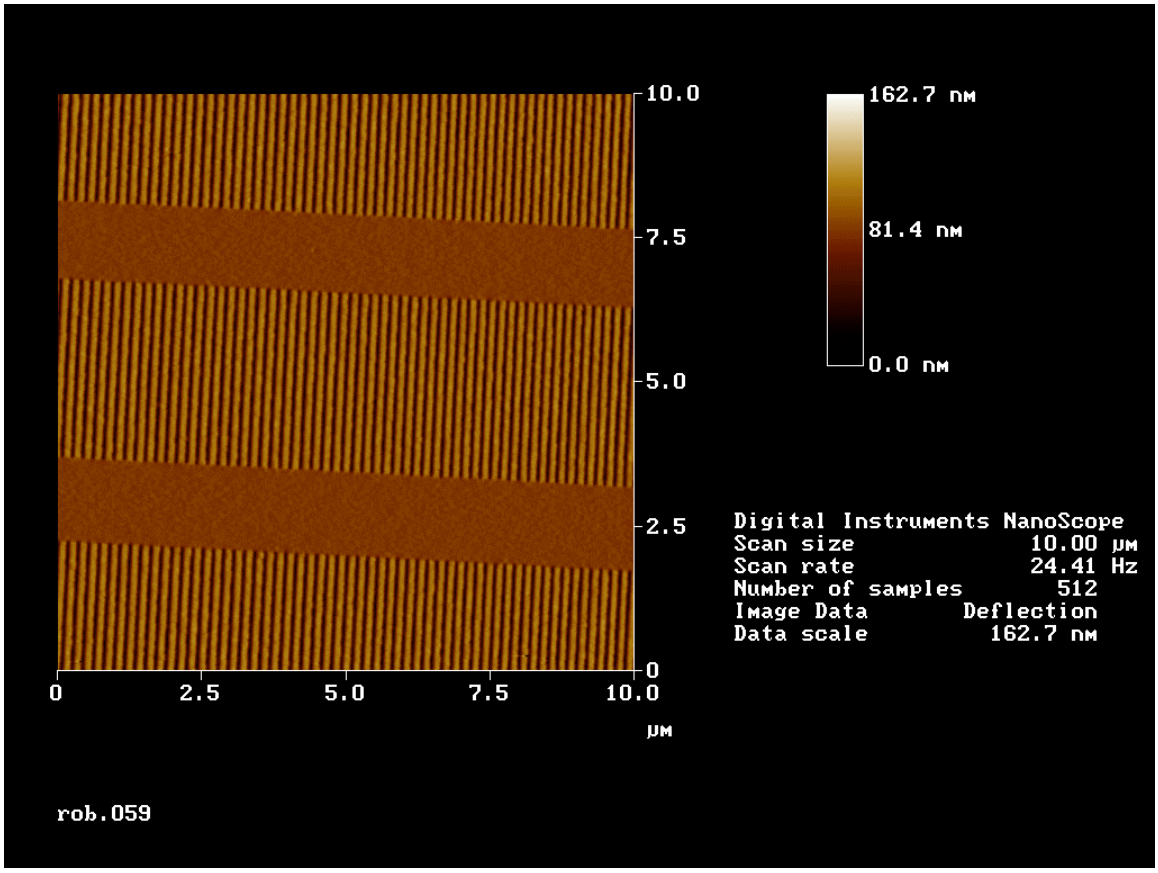

NEXT STEPS IN EXPERIMENTS

Even though the Talbot effect works with any species of atoms or molecules, the goal of lithography creates a few limitations in an experiment. The substance must be able to adhere well to the substrate and not be too mobile because of the small distances involved and the possibility for destructive imaging. Also, since the incident angle generally plays a large role in the resulting intensity pattern, the beam must be well collimated. This is usually done by having a high beam intensity come out of the source and pass through collimation slits, minimizing the effect of the large angular distribution of an extended source. The next step would be to carry out an experiment to deposit rows of atoms onto a substrate. First, one would put the substrate directly behind the grating without the spacers seen in figure 28, to test the substance mobility and the imaging capabilities with an AFM. Once that works, placing spacers with a thickness equal to one Talbot length between the grating and substrate would be the logical next step before attempting to deposit fractional revivals. One might even want to tilt the substrate at an angle relative to the grating, which can guarantee that some part of the substrate will be positioned exactly at the desired distance from the grating.

Fig. 28

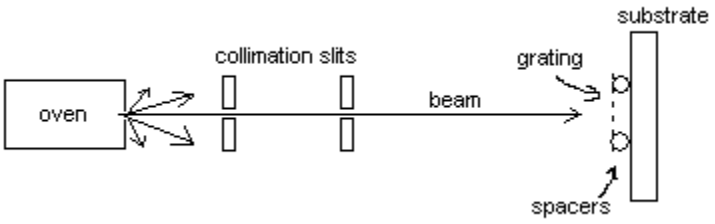

CONCLUSION

Because of the advantages that Talbot-assisted lithography has over optical techniques, it would be beneficial to investigate the possibility further. This research has shown that a number of things must be considered when attempting to deposit atoms onto a substrate by means of Talbot-reconstructed images. The open fraction of the transmission grating plays a very large role in the resulting intensity distribution, especially for the fractional revivals. Smaller open fractions result in well-defined and high-contrast fractional revivals, while large open fraction gratings yield poor contrast for fractional Talbot revivals. Although atoms do interact with the grating walls by means of van der Waals forces, this research has shown that, for purposes of simple atom lithography, these interactions can basically be disregarded. However, a very important factor to consider is the spread in velocities. If that is too great, like a purely thermal beam, one has little hope of creating high contrast structures. Fortunately, there are techniques that effectively narrow the beam velocity spread, such as the use of supersonic expansion. The ideal situation would be to use an atom laser, since that has an extremely narrow velocity distribution, which would create very well-defined patterns. Because of its similarity to the effects of a velocity distribution, beam collimation needs to be controlled to better than $\theta = d/z_T$. Imaging such deposited patterns work very well through the use of an AFM, as long as the atoms do not move around the surface easily. Of course, there are many variations with which such an experiment can be carried out, but I hope that the results of this paper will be of help when considering the details of such an undertaking.

APPENDIX A

All the computer simulations in this thesis were performed with Igor Pro version 4.01. This first section shows the basic code used for most of the simulations. Half_num_slits and half_w_size changes the number of slits and width of the window, respectively, and dimensions are given in nanometers.

```
#pragma rtGlobals=1            // Use modern global access method.

macro dog()                          //  macro to run the talbot program at several different z.
variable z = 0, zT = (100^2)/.01
z =  .01*zT
do
  talbot(z)
  z +=.01*zT
while ( z < 2.51*zT)
end

function  talbot(z)
variable z
string zname;  sprintf zname, "pl%g",z;  make/o/N=200 $zname
variable nr, xx, i=0, n, ww, knr ,snr, vdW
variable d=100,  k = (2*pi/.01),  half_num_slits = 40/2 ,  half_w_size = 70/2
make/o/d/N=200 Inten, x_pos
make/o/N=200/c temp
temp = 0

do                                   // loop over x-position
xx = i*1;  x_pos[i] = xx
n= -half_num_slits

do                                   // loop over number of slits
  ww= -half_w_size

  do                                  //  loop over each window of size ww
   vdW= 0 * ((ww + 0.001 - half_w_size)^-3 - (ww + 0.001+ half_w_size)^-3)
                                     // phase shift due to van der Waals
   nr =  (z+   .5*(xx + n*d+ ww)^2/z )   // parabolic wavefront approx
   knr =k * nr    + vdW
```

```
  snr = sqrt(nr)
   temp[i] += cmplx(cos(knr)/snr, sin(knr)/snr)

ww +=1                          // iterate over points in a single window
  while(ww<half_w_size)

n+=1                            // iterate slit number
 while(n<half_num_slits)

i += 1                          // iterate x-position
while (i<100)

Inten =  magsqr(temp)
duplicate/o Inten $zname
end
```

To sum over a velocity distribution, I simply added a loop to sum over the different velocities in the Talbot function:

```
function  talbot(z,sigma)
variable z, sigma
string zname;  sprintf zname, "%gpl%g",sigma,z;  make/o/N=200 $zname
variable nr, xx, i=0, n, ww, knr, snr, vdW, v, k, prob, sig, v_avg, vmax
variable d=100,  half_num_slits = 40/2 ,  half_w_size = 70/2
make/o/d/N=200 Inten, x_pos
make/o/N=200/c temp

sig = sigma
v_avg = 1500
v = v_avg - 2*sig
vmax = v + 4*sig + 1
Inten = 0

do                              //loop over velocities in m/s
temp = 0
i = 0
prob = exp(-((v-v_avg)^2)/(2*sig^2))/sqrt(2*pi*sig)          //Gaussian distribution
k = 2*pi*v/15

do                              // loop over x-position
xx = i*1;  x_pos[i] = xx
```

```
n= -half_num_slits

do                                  // loop over number of slits
 ww= -half_w_size

 do                                 //  loop over each window of size ww
  vdW= 0 * ((ww + 0.001 - half_w_size)^-3 - (ww + 0.001+ half_w_size)^-3)
                                    // phase shift due to van der Waals
  nr =  (z+   .5*(xx + n*d+ ww)^2/z )   // parabolic wavefront approx
  knr =k * nr  + vdW
  snr = sqrt(nr)
   temp[i] += cmplx(cos(knr)/snr, sin(knr)/snr)

   ww +=1                                   // iterate over points in a single window
  while(ww<half_w_size)

 n+=1                                       // iterate slit number
 while(n<half_num_slits)

Inten[i] += prob*magsqr(temp[i])
i += 1                                      // iterate x-position
while (i<100)

v+= 0.02*sig                                //iterate velocity
while (v < vmax)

duplicate/o Inten $zname
end
```

This is the brute-force method of computing the effects of velocity spread and turns out to be very time-consuming. A more efficient way would be to calculate the carpet for a single velocity, and then stretch or compress it in the *z* direction to create a carpet corresponding to a different velocity. One would have to calculate the carpet with the longest Talbot distance first, and then compress it stepwise in order to preserve detail. The resulting sum, of course weighted by a Gaussian, should look like the distribution from the code shown above, while taking a lot less time to calculate.

APPENDIX B

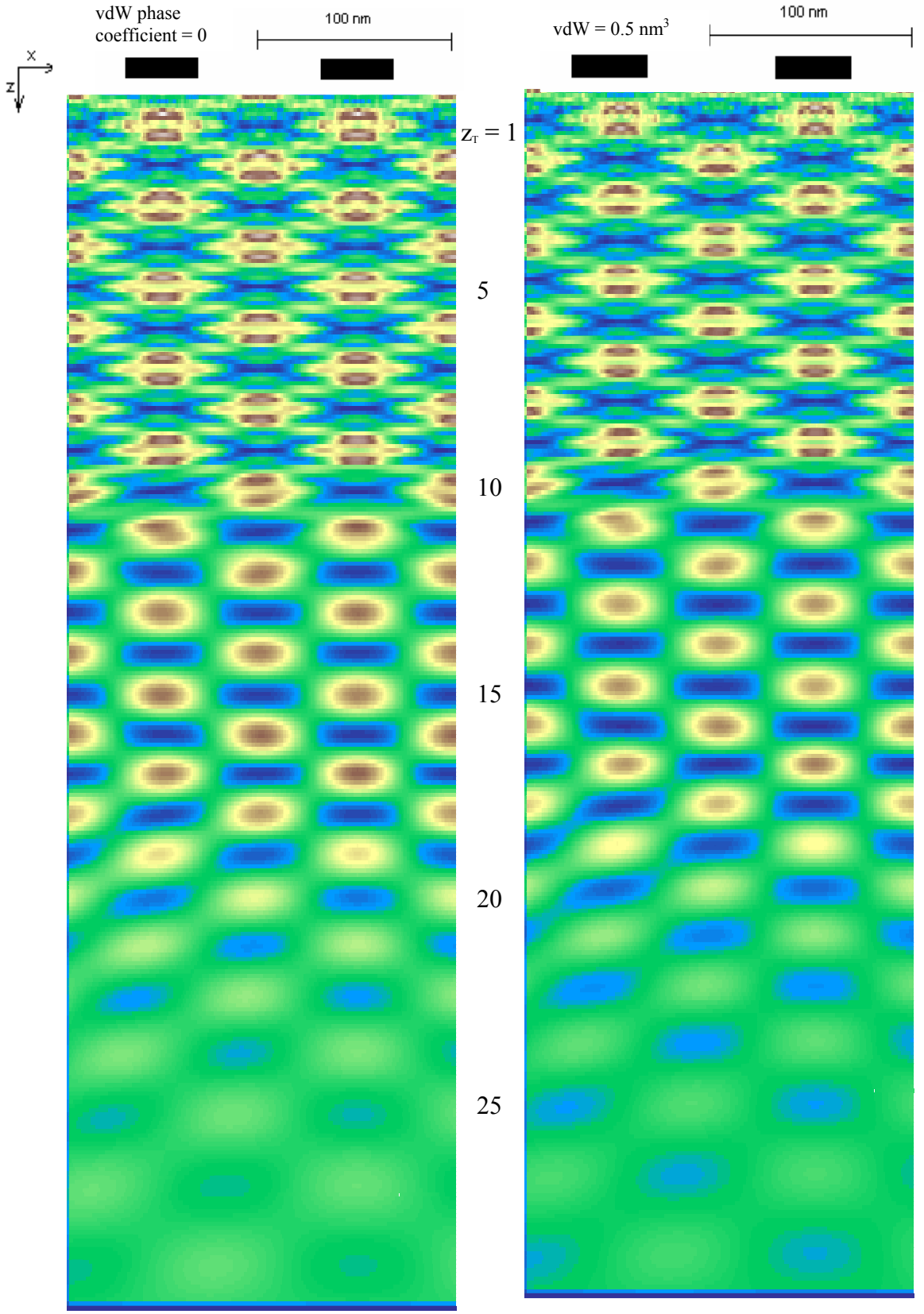
vdW phase
coefficient = 0
100 nm
vdW = 0.5 nm3
100 nm
X
Z
zT = 1
5
10
15
20
25

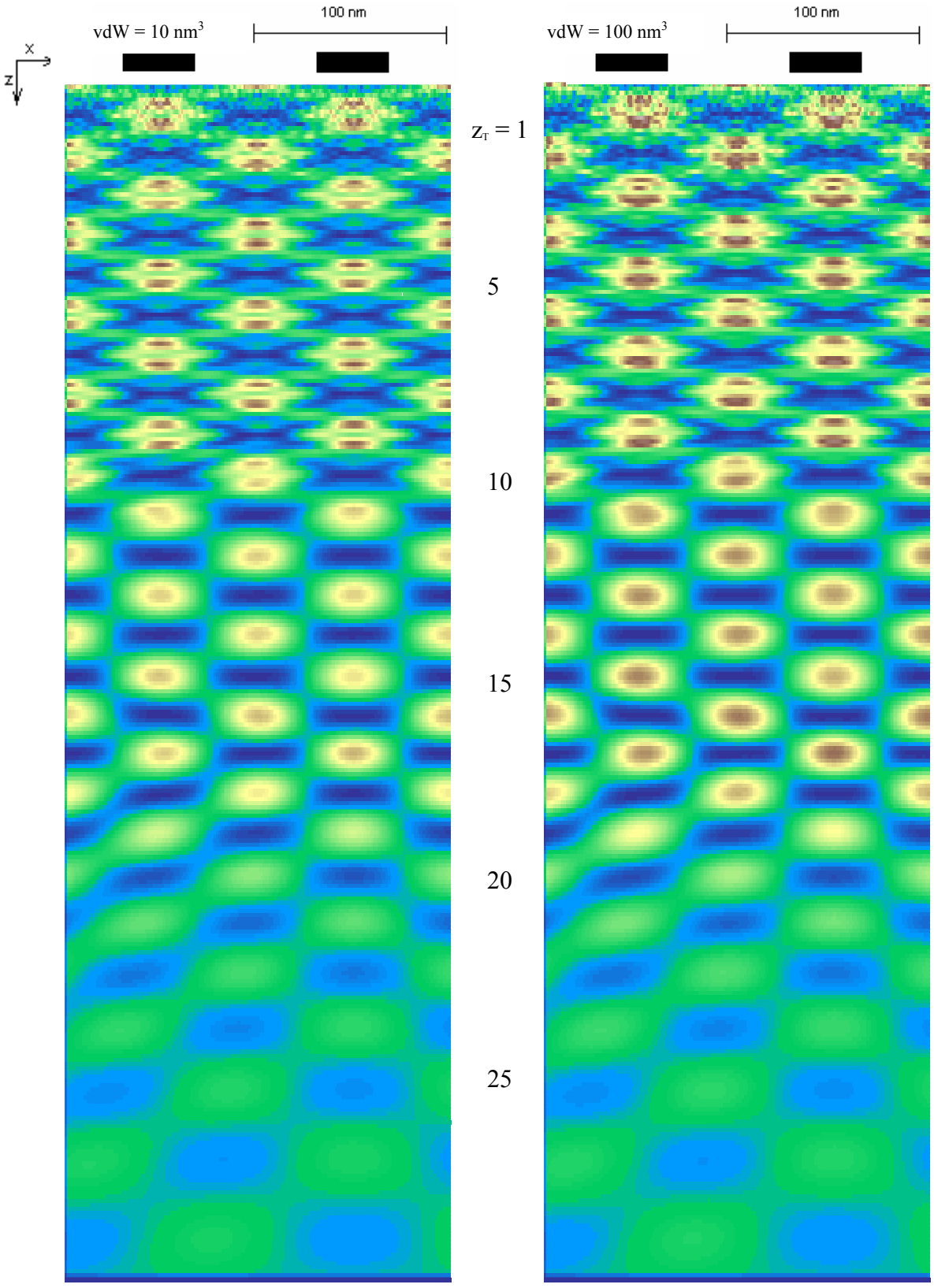
vdW = 10 nm3
100 nm
vdW = 100 nm3
100 nm
X
Z
zT = 1
5
10
15
20
25

ACKNOWLEDMENTS

I would like to thank Dr. Alex Cronin for all his support throughout the whole of this project. His help and guidance was instrumental in its realization, and I could not have done it without him.

---

[1] M. Kanellos, "New Pentium 4 to alter Competitive Map," http://news.com.com/2100-1001-800008.html?legacy=cnet.
[2] R. Leggat, "Talbot, William Henry Fox," http://www.rleggat.com/photohistory/history/talbot.htm, (2000).
[3] J.J. O'Connor and E.F. Robertson, "William Henry Fox Talbot," http://www-gap.dcs.st-and.ac.uk/~history/Mathematicians/Talbot.html, (1997).
[4] Bernd Rohwedder, "Atom Optical Elements Based on Near-field Grating Sequences," Fortschr. Phys. **47** 9-10, 883-911 (1999).
[5] M.S. Chapman, C.R. Ekstrom, T.D. Hammond, J. Schmiedmayer, B.E. Tannian, S. Wehinger, and D.E. Pritchard, "Near-field imaging of atom diffraction gratings: The atomic Talbot effect," Phys. Rev. A **51**, 18 (1995).
[6] S. Nowak, Ch. Kurtsiefer, T. Pfau, and C. David, "High-order Talbot fringes for atomic matter waves," Optics Lett. **22**, 1430 (1997).
[7] J.F. Clauser and S. Li, "Talbot-von Lau atom interferometry with cold slow potassium," Phys. Rev. A **49**, R2213 (1994).
[8] G.S. Spagnolo and D. Ambrosini, "Talbot effect application: measurement of distance with a Fourier-transform method," Meas. Sci. Technol. **11**, 77-82 (2000).
[9] G. Timp, M. Prentiss, R.E. Behringer, D.M. Tennant, J.E. Cunningham, and K.K. Berggren, "Using light as a lens for submicron, neutral-atom lithography," Phys. Rev. Lett. **69**, 1636 (1992).
[10] J.J. McClelland, R. Gupta, Z.J. Jabbour, and R.J. Celotta, "Laser focusing of atoms for nanostructure fabrication," Appl. Phys. Lett. **67**, 1378 (1995)
[11] S.J. Rehse, R.W. McGowan, and S.A. Lee, "Optical manipulation of group III atoms," Appl. Phys. B **70**, 657 (2000).
[12] S.G. Lipson, H. Lipson, D.S. Tannhauser, "Optical Physics," 3rd ed., Cambridge University Press, (1995).
[13] M. Berry, I. Marzoli, W. Schleich, "Quantum carpets, carpets of light," http://physicsweb.org/article/world/14/6/7, (2001).
[14] J.D. Perrault, A. Cronin, and T.A. Savas, "Using atomic diffraction of Na from material gratings to measure atom-surface interactions," (2003).
[15] C. Kittel and H. Kroemer, *Thermal Physics*, 2nd ed., W.H. Freeman and Company, (1980).